

Spring 1995

Classification of Acoustic Emission Signals from an Aluminum Pressure Vessel Using a Self-Organizing Map

Weldon Paul Thornton

Embry-Riddle Aeronautical University - Daytona Beach

Follow this and additional works at: <https://commons.erau.edu/db-theses>



Part of the [Structures and Materials Commons](#)

Scholarly Commons Citation

Thornton, Weldon Paul, "Classification of Acoustic Emission Signals from an Aluminum Pressure Vessel Using a Self-Organizing Map" (1995). *Theses - Daytona Beach*. 198.

<https://commons.erau.edu/db-theses/198>

This thesis is brought to you for free and open access by Embry-Riddle Aeronautical University – Daytona Beach at ERAU Scholarly Commons. It has been accepted for inclusion in the Theses - Daytona Beach collection by an authorized administrator of ERAU Scholarly Commons. For more information, please contact commons@erau.edu.

**CLASSIFICATION OF ACOUSTIC EMISSION SIGNALS FROM AN
ALUMINUM PRESSURE VESSEL USING A SELF-ORGANIZING MAP**

by

Weldon Paul Thornton

A Thesis Submitted to the Graduate Studies Office
in Partial Fulfillment of the Requirements for the Degree of
Master of Science in Aerospace Engineering

Embry-Riddle Aeronautical University
Daytona Beach, Florida
Spring 1995

UMI Number: EP31938

INFORMATION TO USERS

The quality of this reproduction is dependent upon the quality of the copy submitted. Broken or indistinct print, colored or poor quality illustrations and photographs, print bleed-through, substandard margins, and improper alignment can adversely affect reproduction.

In the unlikely event that the author did not send a complete manuscript and there are missing pages, these will be noted. Also, if unauthorized copyright material had to be removed, a note will indicate the deletion.

UMI[®]

UMI Microform EP31938
Copyright 2011 by ProQuest LLC
All rights reserved. This microform edition is protected against
unauthorized copying under Title 17, United States Code.

ProQuest LLC
789 East Eisenhower Parkway
P.O. Box 1346
Ann Arbor, MI 48106-1346

Copyright by Weldon Paul Thornton 1995

All Rights Reserved

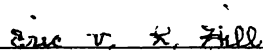
**CLASSIFICATION OF ACOUSTIC EMISSION SIGNALS FROM AN
ALUMINUM PRESSURE VESSEL USING A SELF-ORGANIZING MAP**

by


Weldon Paul Thornton

This thesis was prepared under the direction of the candidate's thesis committee chairman, Dr. Eric v. K. Hill, Department of Aerospace Engineering, and has been approved by the members of his thesis committee. It was submitted to the Department of Aerospace Engineering and was accepted in partial fulfillment of the requirements for the degree of Master of Science in Aerospace Engineering

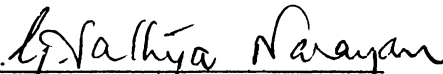
THESIS COMMITTEE



Dr. Eric v. K. Hill
Chairman



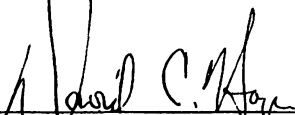
Dr. Frank Radosta
Member



Dr. Sathya Gangadharan
Member



Coordinator, MSAE Program



Department Chair, Aerospace Engineering

6/5/95
Date

ACKNOWLEDGMENTS

I would first like to thank my wife Coleen. Her constant understanding and support helped me complete this research. Next, I would like to thank my thesis advisor, Dr. Eric v. K. Hill. His patience and guidance gave me motivation and direction throughout this research. I would also like to thank Dr. Frank Radosta and Dr. Sathya Gangadharan for serving on the thesis committee. A special thanks goes to my parents who inspired me to go to college and whose encouragement stayed strong throughout my college years. I would also like to thank Mike Marsden, Rob Demeski, Jennifer Turner, and Dana Lamborn for their assistance on this research. Last, but definitely not least, I am extremely grateful to Dr. T. David Kim who gave me the chance to prove myself in graduate school.

ABSTRACT

Author: Weldon Paul Thornton
Title: Classification of Acoustic Emission Signals from an Aluminum Pressure Vessel Using a Self-Organizing Map
Institution: Embry-Riddle Aeronautical University
Degree: Master of Science in Aerospace Engineering
Year: 1995

Acoustic emission nondestructive testing has been used for real-time monitoring of complex structures. All of the structures were made of materials at least 0.070 inch thick. The purpose of this research was to demonstrate the feasibility of using neural networks to classify acoustic emission signals gathered from a pressure vessel made of 2024-T3 aluminum 0.040 inches thick, i.e. thin aluminum sheet. AE waveforms were recorded during fatigue cycling of one pressure vessel using a wide band transducer and a digital oscilloscope connected to a computer. The source for each signal was determined using two narrow band transducers and a LOCAN-AT data acquisition system. The power spectrum was calculated for each waveform. A Kohonen self-organizing map (SOM) was used to cluster the spectra. The network clustered the data on a two-dimensional feature space according to the source of the signal. A total of 3,600 power spectra were used to train the neural network, and 1,800 were used to test the network. Initially there was overlap between the clusters on the two-dimensional feature space; however, this was found to be due to human error. The SOM itself correctly classified all of the signals.

TABLE OF CONTENTS

	Page
Copyright	ii
Signature Page	iii
Acknowledgments	iv
Abstract	v
Table of Contents	vi
List of Tables	viii
List of Figures	ix
CHAPTER 1 INTRODUCTION	1
1.1 General Overview	1
1.2 Previous Research	2
1.3 Current Approach	3
CHAPTER 2 BACKGROUND THEORY	5
2.1 Acoustic Emission	5
2.1.1 Phenomenology	6
2.1.2 Application to Metal Fatigue Detection	7
2.1.3 Effects of Dispersive Mediums	8
2.2 Neural Networks	10
2.2.1 Neural Network Applications and Learning Methods	11
2.2.2 Neural Network Architecture	12
2.2.3 Previous Research	14
CHAPTER 3 EXPERIMENTAL APPARATUS AND TESTING PROCEDURE	16
3.1 Experimental Apparatus	16
3.1.1 Pressure Vessel	16
3.1.2 Pressurization System	18
3.1.3 Sensors	19
3.1.4 Data Acquisition	22
3.2 Data Conditioning	24
3.2.1 Preprocessing	24
3.2.2 Bandwidth Requirements	26
3.3 Testing Procedure	27
CHAPTER 4 NEURAL NETWORK ARCHITECTURE, OPERATION, AND IMPLEMENTATION	30
4.1 Selection of a Neural Network	30

4.1.1	Input Data for the Neural Network	30
4.1.2	Justification for Using a Neural Network	32
4.2	Architecture of Neural Network Selected	34
4.3	Neural Network Operation	37
4.4	Neural Network Implementation	41
4.4.1	Selection of Control Parameters	41
4.4.2	Training the Neural Network	43
4.4.3	Testing the Neural Network	44
CHAPTER 5	ANALYSIS AND VERIFICATION OF RESULTS	45
5.1	Preliminary Networks and Their Results	45
5.2	Analysis and Verification of Results	50
CHAPTER 6	CONCLUSIONS AND RECOMMENDATIONS	53
6.1	Conclusions	53
6.2	Recommendations	53

LIST OF TABLES

Table	Page
Table 4.1 SOM Control Parameters	42
Table 4.2 SOM Architecture and Processing Parameters	43

LIST OF FIGURES

Figure	Page
Figure 2.1 Acoustic Emission Sensor	6
Figure 2.2 Frequency Response For Wide Band Sensor	7
Figure 2.3 Spherical AE Wave Propagation	9
Figure 2.4 Acoustic Emission Wave Reflections	9
Figure 2.5 Simple Neural Network	12
Figure 2.6 Processing Element	14
Figure 3.1 Aluminum Pressure Vessel Test Apparatus	17
Figure 3.2 Aluminum Patch for Hole in Cylinder	18
Figure 3.3 Placement of Acoustic Emission Sensor for Rivet Signals	20
Figure 3.4 Placement of Acoustic Emission Sensor for Crack Signals	21
Figure 3.5 Instrumentation Configuration	24
Figure 3.6 Digitized AE Signal	26
Figure 3.7 Linearly Reduced Power Spectrum	26
Figure 3.8 Aliasing of Signal Due to Improper Digital Sampling Rate	27
Figure 3.9 Testing Procedure	29
Figure 4.1 Rivet Signal Power Spectrum	31
Figure 4.2 Rubbing Signal Power Spectrum	31
Figure 4.3 Crack Signal Power Spectrum	31
Figure 4.4 Two Rivet Signals with Different Power Spectra	32
Figure 4.5 Recorded Rivet Signal	33
Figure 4.6 Recorded Rubbing Signal	33
Figure 4.7 Recorded Crack Signal	33
Figure 4.8 Self-Organizing Map General Architecture	35
Figure 4.9 Example of a SOM with Three Classes	36
Figure 4.10 Neighborhood of a Self-Organizing Map	38
Figure 5.1 Preliminary SOM #1	47
Figure 5.2 Preliminary SOM #2	48
Figure 5.3 Final SOM	49
Figure 5.4 General Regions for Mechanisms as Classified by the Final SOM	51
Figure 5.5 Final SOM for Corrected Data	53

CHAPTER 1

INTRODUCTION

1.1 GENERAL OVERVIEW

As the number of aging aircraft increases, the need for systems capable of real-time in-flight structural monitoring grows. A natural problem for aircraft approaching their design lives is the development of fatigue cracks. Fatigue cracks occur in structurally critical areas that can sometimes result in catastrophic losses. One example of this was the Aloha Airlines Boeing 737-200 that lost part of its top front fuselage during flight [O'Lone]. Recognizing that the problem with aging aircraft is growing, a practical solution becomes imperative.

The cost of new aircraft coupled with a depressed aviation industry eliminates the easy solution of replacing all aging aircraft in a timely manner. Thus, the goal of commercial airlines and the military is to replace parts as needed rather than at specified intervals in the design life of the aircraft. As such, there is a large demand for a cost effective, accurate in-flight structural monitoring system. An in-flight monitoring system could be used to implement replacement of parts as needed on new aircraft as well as on aging aircraft. In addition to the reduction of accidents caused by structural failure, the aviation industry could benefit from reduced downtime for aircraft and reduced labor costs for testing aircraft parts.

Acoustic emission (AE) nondestructive testing is a passive testing method that monitors the reaction of a structure to an applied load. This method is often capable of monitoring large areas rather than specific locations; hence, it provides a global monitoring capability. Acoustic emission also monitors structural noise and flaw growth in real-time. Because of these attributes, AE has proven to be the most viable of all nondestructive testing methods for in-flight monitoring.

1.2 PREVIOUS RESEARCH

Several attempts have been made to monitor aircraft structures using acoustic emission nondestructive testing. The results have been varied but are indicative of the potential for AE testing. Acoustic emission testing was used to measure fatigue crack growth on the Canadian C-130 Hercules aircraft with good results [McBride and Maclachlan]. Here the monitoring was of 7075-T6 aluminum sections. The level of in-flight noise was considerable, but identification of crack signals was accomplished nonetheless. A similar application was performed on the 625 aircraft KC-135 fleet. The lower wingskins, constructed of 7178-T6 aluminum, were instrumented with a specially designed AE system that detected unstable crack growth of at least 0.5 inches in length [Parrish]. Another example was the monitoring of fatigue crack growth in a 4330V steel frame from an F-105 [Rodgers]. All of the above in-flight AE tests were involved with monitoring of large amplitude AE signals on thick (greater than 0.070 inches) sections.

The major drawback with most of these tests was that the data analysis and reduction were time consuming, labor intensive, and costly. The goal for a real-time, in-

flight monitoring system is realizable only if a method can be developed to analyze the data and identify the sources of the AE signals in real-time. The above research demonstrated the feasibility of AE nondestructive testing as an in-flight monitoring technique, but recent computer advances may hold the key to real-time data analysis of structural integrity.

1.3 CURRENT APPROACH

In spite of its many benefits, AE testing has not been totally accepted as an in-flight monitoring technique for one main reason: the identification of the AE signals measured on aircraft is very difficult and, up to now, could not be accomplished quickly with a high degree of accuracy. Here it is necessary to sort out crack growth signals from rubbing and rivet fretting signals. Complex structures such as aircraft have a tendency to be very noisy thus complicating the problem of signal identification. Also environmental noise and structural noise can often distort an AE signal beyond easy recognition. The problem becomes even more difficult when AE sources generate signals simultaneously. Hence, the identification of AE signals can be considered a pattern recognition problem.

Research on pattern recognition of AE signals has been conducted at the NASA Langley Research Center for a number of years. Their engineers have been able to identify raw AE signals as either crack growth, rubbing, or rivet fretting with a good deal of accuracy but not without a certain amount of difficulty [Prosser]. Again, the difficulty comes in the area of pattern recognition. In the past few years, neural networks have been developed to perform pattern recognition very rapidly and accurately.

The purpose of this research is to prove the feasibility of using AE nondestructive testing to measure fatigue crack growth on a complex structure made of *thin* aluminum (0.040 inches thick). Classification of the AE signals was accomplished using a neural network. The neural network classified the AE signals as either crack growth, rivet fretting, or metal on metal rubbing.

CHAPTER 2

BACKGROUND THEORY

2.1 ACOUSTIC EMISSION

Acoustic emission nondestructive testing can be used to model different failure modes in complex structures. It has several advantages over other methods such as ultrasonic testing or eddy current testing, one of which is that the structure does not have to be removed from service to be tested. AE is a noninvasive testing technique that measures energy waves generated by flaw growth activity within the test specimen as a load is applied. In some cases a single sensor can be used to measure a large portion or even the entire structure, depending on the geometry and type of material of which the structure is constructed. This is called global monitoring. Other methods are more localized in their coverage and need to either generate an energy field or use special chemicals to probe for flaws. For example, radiography employs X-rays and gamma rays to image subsurface flaws, while liquid penetrant testing uses dyes to visually check for surface breaking flaws in a structure. Acoustic emission cannot image flaws; it only senses their growth when a load is applied. Analysis of this flaw growth data can provide both a qualitative and a quantitative measure of structural integrity.

2.1.1 PHENOMENOLOGY

An AE event occurs as a result of a rapid release of strain energy within a stressed material. The source of this energy release in metal structures can be crack growth, metal on metal rubbing, fastener fretting, or some external source. The energy released is in the form of stress wave packets that radiate spherically outward from the source through the material to the surfaces. On the surface of structures the stress wave packets appear in the form of vibrations. The monitoring of these stress waves requires special sensors.

Acoustic emission sensors typically use a piezoelectric element to convert the stress waves into electrical signals. They can detect very small surface vibrations over a wide range of frequencies. Piezoelectric transducers are available in two basic types, resonant and non-resonant. These sensors are also available in different bandwidths. For example, the Physical Acoustics Corporation (PAC) R30 sensors used herein have a response bandwidth from 200 KHz to 400 KHz. Non-resonant sensors have a wider response bandwidth, generally from 100 KHz to 1.2 MHz. A generic diagram for a nonresonant or wide band AE sensor is presented in Figure 2.1.

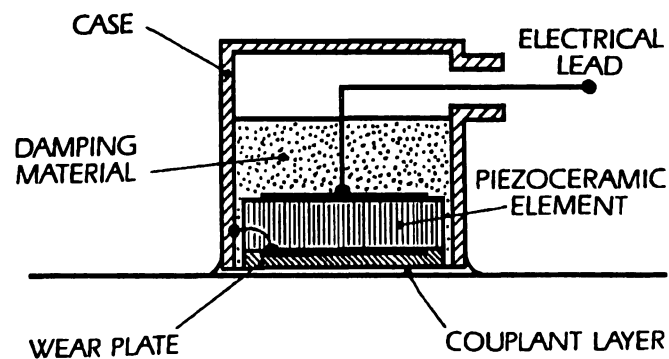


Figure 2.1 Acoustic Emission Sensor

The classification of a sensor as narrow band or wide band depends on the response of the sensor to various frequencies. A response graph is typically provided with each sensor that is purchased. Figure 2.2 shows the response for the PAC WDI wide band sensor employed in this research.

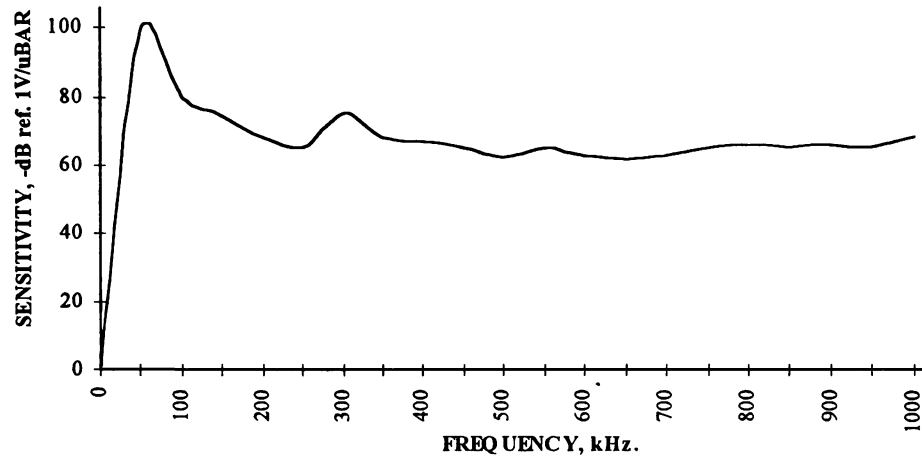


Figure 2.2 Frequency Response For Wide Band Sensor

2.1.2 APPLICATION TO METAL FATIGUE DETECTION

Acoustic emission testing has been used to detect the initiation and propagation of cracks in fatigued materials. It has also been used to monitor low cycle fatigue of metals. Low cycle fatigue is when the structure fails in less than 10,000 cycles due to extremely high stress levels. AE testing has also been used in high cycle fatigue tests which is when failure of the structure occurs after more than 10,000 cycles. During high cycle fatigue tests AE has been used to detect crack initiation and formation but not to monitor the actual fatigue process.

2.1.3 EFFECTS OF DISPERSIVE MEDIUMS

The propagation of an AE wave varies according to the geometry of the structure and the material from which it is constructed. In metals there are a number of factors involved in the attenuation of the AE wave. A few of the more influential factors are the thickness of material, material properties, frequency of the AE wave, distance of the sensor from the wave, and interfaces with the boundaries of the structure.

Dispersion is a form of wave attenuation that is affected by the material properties, the distance the wave travels, and the frequency of the wave. It decreases the amplitude and increases the duration of the signal. As the wave travels through a material, the velocity for each frequency component is different, which results in a wave-like signal as opposed to the burst-like emission that is generated by crack initiation or crack propagation. In addition to dispersion, other factors to be included in wave attenuation are geometric spreading, scattering and diffraction, and other energy loss mechanisms.

Geometric attenuation is the decrease in amplitude of an AE wave as it travels through a material. In an ideal case, there would be no loss of energy as the wave traveled, but the amplitude would decrease because a constant amount of energy is being spread over a spherical surface that increases in size as shown in Figure 2.3.

Energy lost to the material in which the AE wave is traveling is a problem that is common to real systems as compared to ideal systems. The wave can be considered as mechanical energy that will experience losses unless the medium through which it is traveling is perfectly elastic. There are no perfectly elastic structures in the real world,

and therefore, the mechanical energy of the wave experiences losses due to the deformation of the material as the wave propagates from the source. Mechanical energy can also be converted to thermal energy which is another form of energy loss. The result is that the AE wave will lose energy regardless of which mechanism is acting.

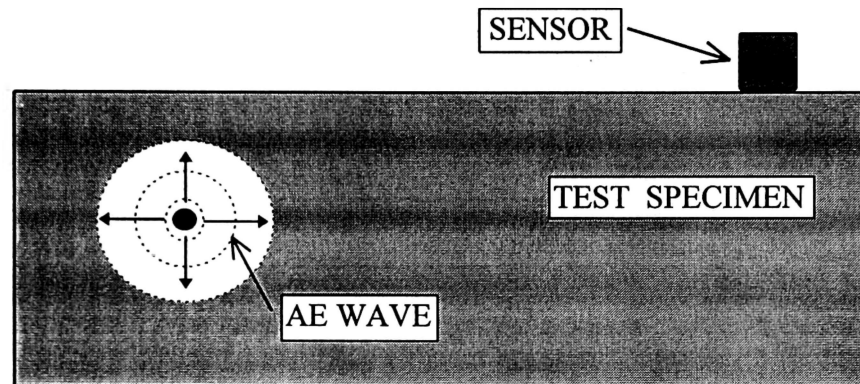


Figure 2.3 Spherical AE Wave Propagation

Aluminum exhibits strong attenuative and dispersive properties. Wave propagation in thin aluminum (0.040 inches thick) would be even more difficult to analyze due to wave reflection and dispersion at interfaces with either air or other metals.

Figure 2.4 shows paths of travel by reflections within a plate.

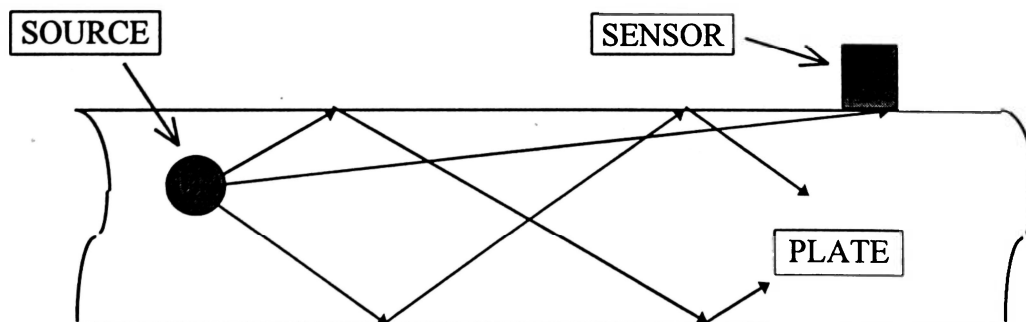


Figure 2.4 Acoustic Emission Wave Reflections

Attenuation from scattering and diffraction is common in structures with complex boundaries and discontinuities such as holes, cracks, or inclusions. The wave traveling through the material interacts with the discontinuity, and the result is a scattering of the wave. The wave reflects in many different directions which decreases its overall amplitude. In some cases, such as with a crack or a groove, it is possible for the wave to reflect and some of the energy to be diffracted around the crack region. In summary, because of all of the above effects, it is believed that AE monitoring of complex aerospace structures would be problematical, and classification of the signals could be extremely difficult.

2.2 NEURAL NETWORKS

Neural networks came from computer research oriented towards modeling the human brain. The level of information processing and problem solving abilities that the human brain processes is a desirable attribute for computers. Neural networks have been applied to a variety of tasks such as speech and text recognition, multivariate statistical analysis, prediction of the stock market, and diagnosis of illness. A drawback to neural networks is that they are often limited to solving one specific type of problem such as prediction or classification. However, some networks are capable of solving multiple problems (such as prediction and classification) simultaneously.

2.2.1 NEURAL NETWORK APPLICATIONS AND LEARNING METHODS

In general, there are six different applications for neural networks [Neuralware].

Each application is briefly described below. Note that there is some overlap in the applications and that each particular application is dependent on the input data and the desired output. The overlap between applications can be attributed to the flexibility of neural networks. Neural networks are oftentimes sufficiently flexible that small changes in the internal processes of a particular network allow the application of that same network to a different problem.

Classification:	Input values are used to assign a category or class.
Prediction:	Input values are used to predict the output value(s).
Data Association:	Network learns from ideal input data to assign a category or class to noisy input data. This is very similar to classification networks except that ideal data is needed to train the network.
Data Conceptualization:	Data are analyzed and conceptual relationships are determined.
Data Filtering:	Smooth a noisy input signal.
Optimization:	Determine optimal values.

Neural networks require iterative feedback training, much as a child when its learning to talk. Some networks use supervised training, and other networks use unsupervised training. Supervised training requires the network to be told what answer it should generate for each given input, while unsupervised training does not require any additional information other than the input data. In general, classification, prediction, and data association require supervised training, whereas data conceptualization, data filtering, and optimization use unsupervised training. There are some cases where a network type

that normally requires supervised training can actually use unsupervised training. An example of this is a self-organizing map, which is a classification network that uses unsupervised training to categorize input data.

2.2.2 NEURAL NETWORK ARCHITECTURE

A neural network can be broken down into three general layers known as the input layer, the processing or mapping layer, and the output layer. The input layer accepts the input data and distributes it to the processing layer. The processing layer can consist of several layers as required by the complexity of the problem. Normally processing is conducted with either one or two layers, but as many as four have been used. These layers, which are used for the majority of processing, are also referred to as hidden layers. Finally, the output layer yields the desired information. Figure 2.5 shows a simple, three layer neural network with each circle representing a processing element (PE) or artificial neuron. To better understand how a neural network functions, it is necessary to review how a PE performs.

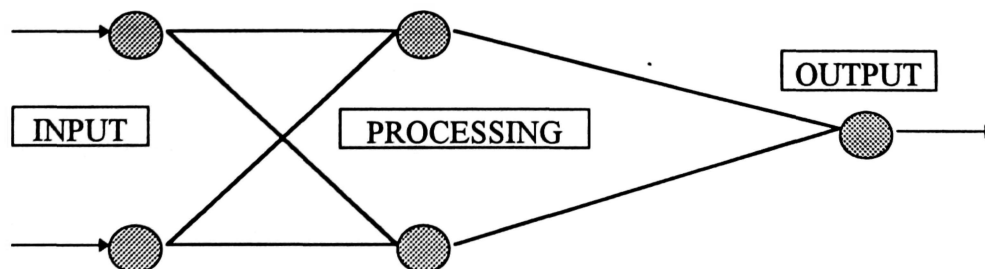


Figure 2.5 Simple Neural Network

A PE has a central element and connections. Each connection represents a path over which the data will travel. It also has a multiplication factor to adjust the values of the data. The multiplication factor is known as a weight and typically has a value between 0 and 1. The more important the data on a given connection, the higher the weight value. The central element performs either one or two functions. First, it will sum the data values after the weights have been applied; then if there is a second function, it will perform that as well. The second function is called a transfer or activation function. It is a nonlinear mathematical expression that is applied to the resultant of the summation function. Figure 2.6 shows a PE with its weights and connections.

A neural network can consist of literally hundreds of PE with thousands of connections. With each connection being a weighted multiplication of its input and each PE including either one or two mathematical operations, it is not practical to perform these operations manually; rather, they are performed on a computer. The resultant combination of all the PE is a neural network capable of learning very complex and labor intensive tasks in a relatively short period of time. If the input changes, the network needs only to be retrained with data that includes the changes.

One benefit of neural networks over other computer methods is that occasionally an erroneous number may be placed in the input data or a PE may become nonfunctional, yet the network can still perform its desired function. This is called fault tolerance, which is unlike standard computer programs that have very little, if any, tolerance for incorrect input data or an error in the program. Also neural networks can suffer from degradation or loss of multiple PE with only a small penalty in performance.

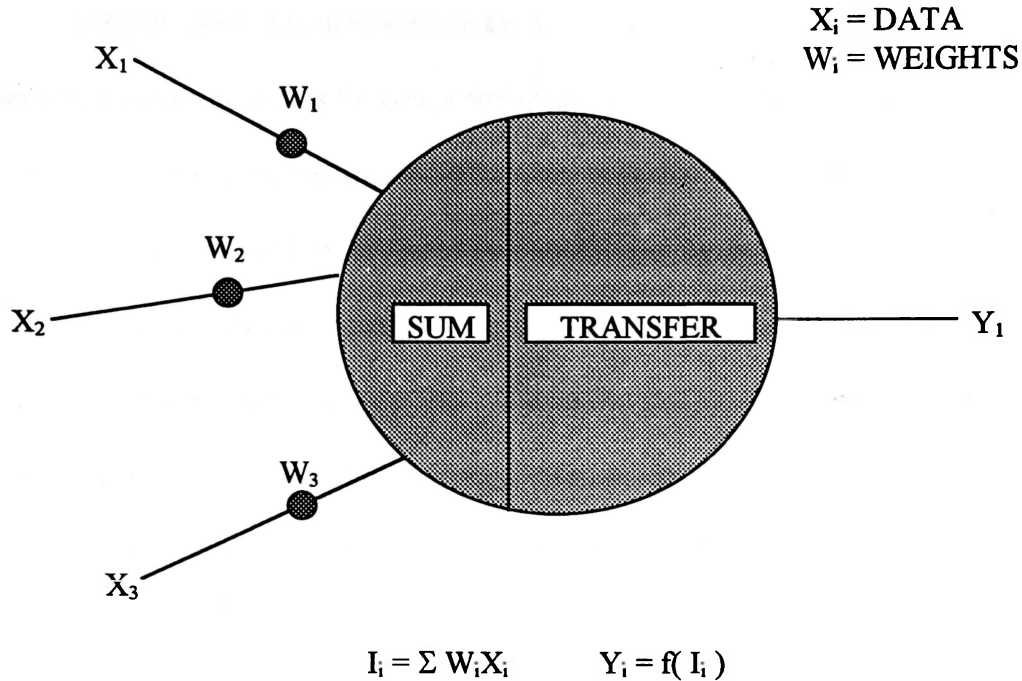


Figure 2.6 Processing Element

2.2.4 PREVIOUS RESEARCH

The use of neural networks has varied from the identification of objects from sonar data to prediction of stock market trends. Application of neural networks to nondestructive testing is increasing steadily even though there has been some resistance. It is a common belief that neural networks are somewhat of a black art. Only through real applications and numerous research projects has the use of neural networks for data analysis gained acceptance. Neural networks have been applied to acoustic emission nondestructive testing data. The solutions include both classification and prediction problems.

A supervised prediction network known as backpropagation was used to determine ultimate strengths for composite pressure vessels [Hill, Walker, and Rowell]. The application of neural networks to composite pressure vessels was useful in proving that burst pressures could be calculated by proof testing the bottles at less than 25% of their expected ultimate load rather than at current proof testing pressures which are at least 70% of the expected ultimate load. It is known that loading some composite pressure vessels over 25% of their expected ultimate loads causes structural degradation and may result in premature failure of the vessels at loads less than ultimate. Another use for a backpropagation network was the prediction of aluminum-lithium weld strengths from acoustic emission data collected during testing of the welds [Hill, Israel, and Knotts]. The prediction of ultimate strengths in the welds was completed with errors of less than 3%. While both of these applications were very successful, the problem of interest here was not prediction but classification.

An unsupervised neural network known as a self-organizing map (SOM) has been used to classify the failure mechanisms present during testing of graphite-epoxy tensile test specimens [Ely]. The SOM clusters similar data to indicate trends. Six failure mechanisms were classified and identified. It was decided that this same type of network would be used in this research in an effort to sort out crack growth AE signals from rubbing and rivet fretting signals.

CHAPTER 3

EXPERIMENTAL APPARATUS AND TESTING PROCEDURE

3.1 EXPERIMENTAL APPARATUS

3.1.1 PRESSURE VESSEL

The pressure vessel used for this project was constructed of two steel endplates with rubber sealing pads and 0.040 inch thick 2024-T3 aluminum sheet rolled into a cylinder (Figure 3.1). A PVC bladder was used to keep the vessel from leaking. The system was held together with twelve, 5/8-inch diameter, threaded rods. On the outer side of each endplate, there was a reinforcing brace to keep the endplate from deforming. One endplate had three threaded holes in it that allowed the attachment of a pressure transducer, a pressure gage, and a filling port. The other endplate had a single hole to attach the hose from the hydraulic pump which pressurized the vessel.

The aluminum vessel was 12 inches long and 12 inches in diameter. The rolled sheet had a two-inch, overlapped, riveted joint. The joint contained two lines of rivets. The distance between the two lines of rivets was 0.625 inches. The spacing between the rivets of each line was 0.4 inches. A one-inch diameter hole was cut through the skin of the vessel, and a notch was filed at the edge of the hole, parallel to the cylinder axis. The notch induced a stress concentration from which a fatigue crack propagated. A PVC

lining was placed over the inside surface of the vessel to keep the PVC bladder from rubbing against the rivets and to reduce extraneous noise. The bladder contained the water used to pressurize the vessel. An aluminum patch was riveted on the inside of the cylinder to prevent the bladder and liner from stretching out the one-inch hole (Figure 3.2). A two-inch flap at each end of the bladder overlapped the edges of the cylinder and acted as a seal.

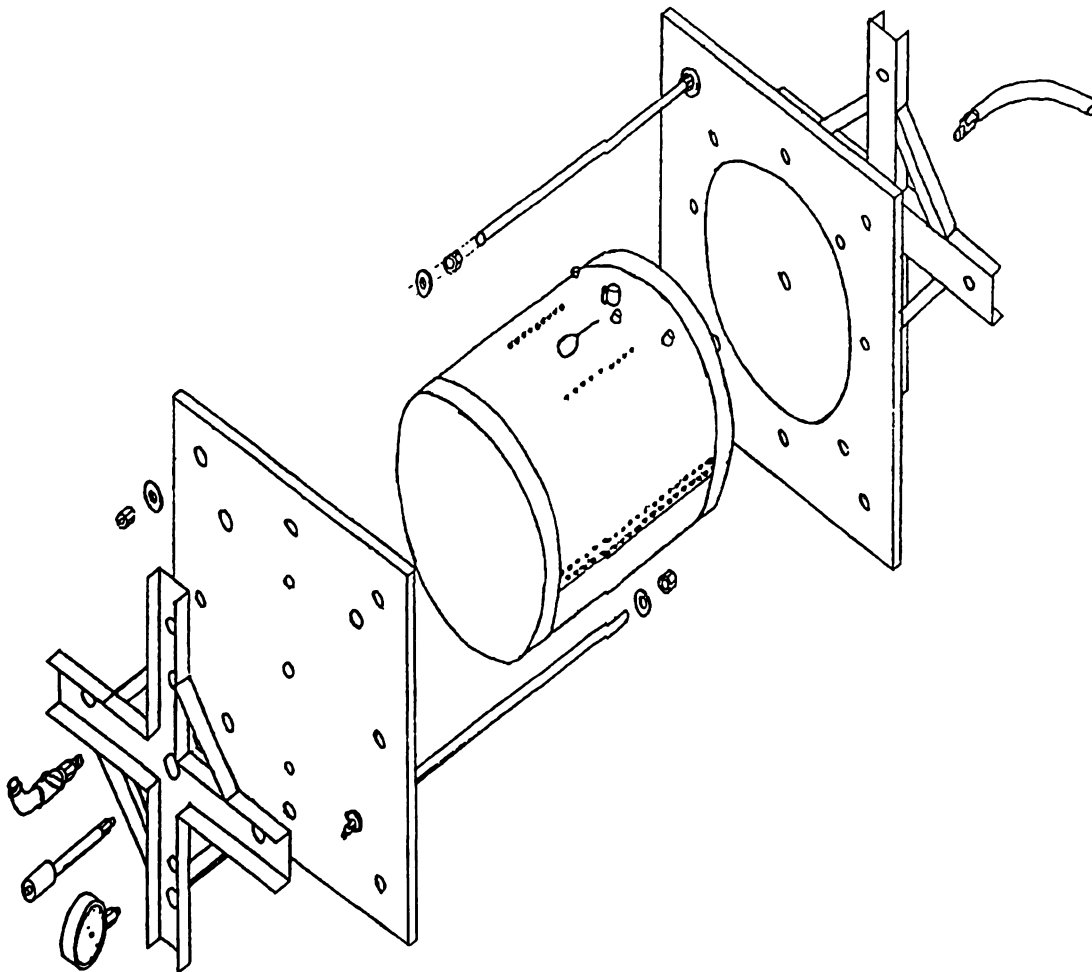


Figure 3.1 Aluminum Pressure Vessel Test Apparatus

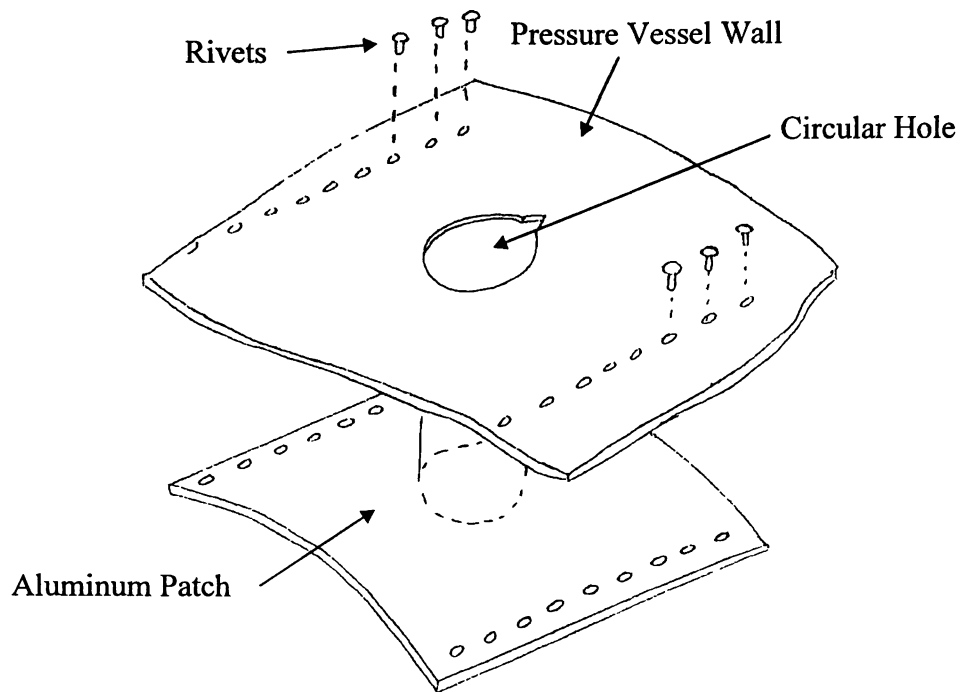


Figure 3.2 Aluminum Patch for Hole in Cylinder

3.1.2 PRESSURIZATION SYSTEM

First, the vessel was filled with water, and any air inside was bled out of the system. Next the vessel was cycled between 0 and 80 psi at 0.5 Hz and then at 1.0 Hz using the water pump that was placed in the grips of the Materials Testing System (MTS) machine. Three tests were performed for each of the two cycling frequencies. Each test consisted of acquiring approximately 520 AE signals. The signals were either from noise, crack growth, rivet fretting, or rubbing. The result was a total of approximately 3,000 AE waves obtained for each source mechanism. The sine function was selected on the MTS 410 Digital Function Generator which resulted in a specified displacement of the piston that corresponded to a sine wave. The amplitude of the sine wave could be

altered by adjusting the span. The set point was adjusted to a pressure of 50 psi and served as the zero point for the sine function.

The MTS is typically used to determine material properties of test specimens. It is capable of applying a force of 10,000 lbs. in tension or compression. The test specimen is placed in a pair of rams, each having a hydraulic grip. The force required to pull a specimen apart may be displayed on the MTS 464 Data Display.

The information from the load cell in the upper ram and the Linear Variable Differential Transformer (LVDT) in the lower ram are collected and displayed by the MTS 464 Data Display. The outputs are displayed on the digital readouts "Input 1" and "Input 2". The display may be programmed to output force in lbs, stress in psi, or displacement in inches. All the information acquired by the system may be printed on a printer linked to the system.

The rate at which a particular MTS function will be performed is controlled by the MTS 410 Digital Function Generator. There are two program rate controls, "Rate 1" and "Rate 2." Rate 1 controls the rate at which the test is performed. For example, the function generator controls the speed of the lower ram during the first half of the ramp function while a tensile test is in progress. For a cyclic test, it controls the frequency of the selected function. Rate 2 controls the rate for the second half of the ramp function and is independent of Rate 1. The 410 Digital Function Generator offers several operating functions including ramp, sine, Haver sine, and Haver square functions.

The MTS 436 Control Unit acts as a toggle switch for the general operation of the MTS and controls other functions as well. The control unit contains the controls for the

set point and the span. As a safety feature, to minimize possible damage or personal injury, there is a hydraulic interlocking system that will engage if the safety door is opened.

3.1.3 SENSORS

Three resonant piezoelectric sensors and a non-resonant (wide band) piezoelectric sensor were used to detect signals from the pressure vessels. The resonant sensors had a frequency range of 200 to 400 kHz. The non-resonant sensor had a frequency range of 100 kHz to 1.2 MHz. Each of the sensors was connected through individual channels to the data acquisition system. All of the sensors were able to detect the signals produced by noise, rubbing, rivet fretting, or cracking. A typical arrangement for the placement of the sensors is shown in Figure 3.3 and 3.4.

- 1 - Recording Sensor, non-resonant
- 2 - Trigger Sensor, resonant
- 3 - Location Sensor 1, resonant
- 4 - Location Sensor 2, resonant

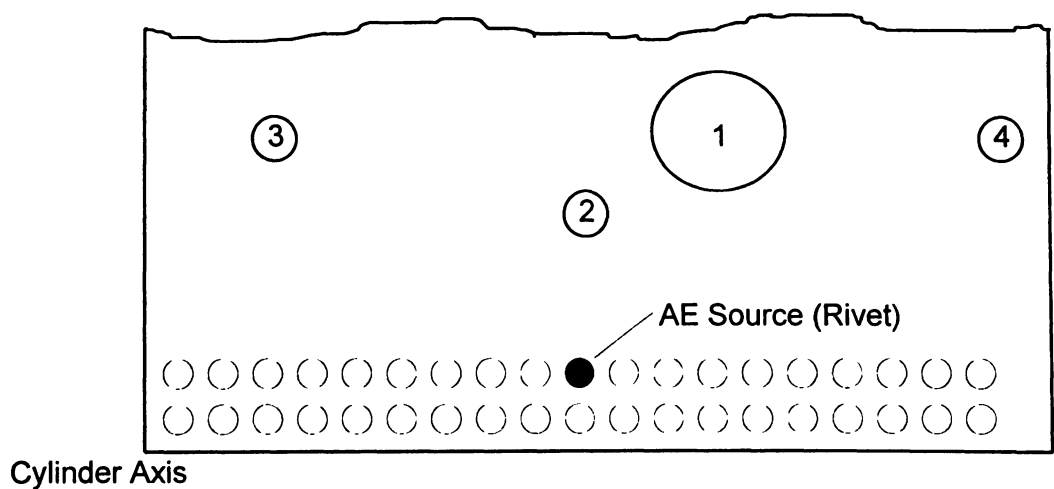


Figure 3.3 Placement of Acoustic Emission Sensor for Rivet Signals

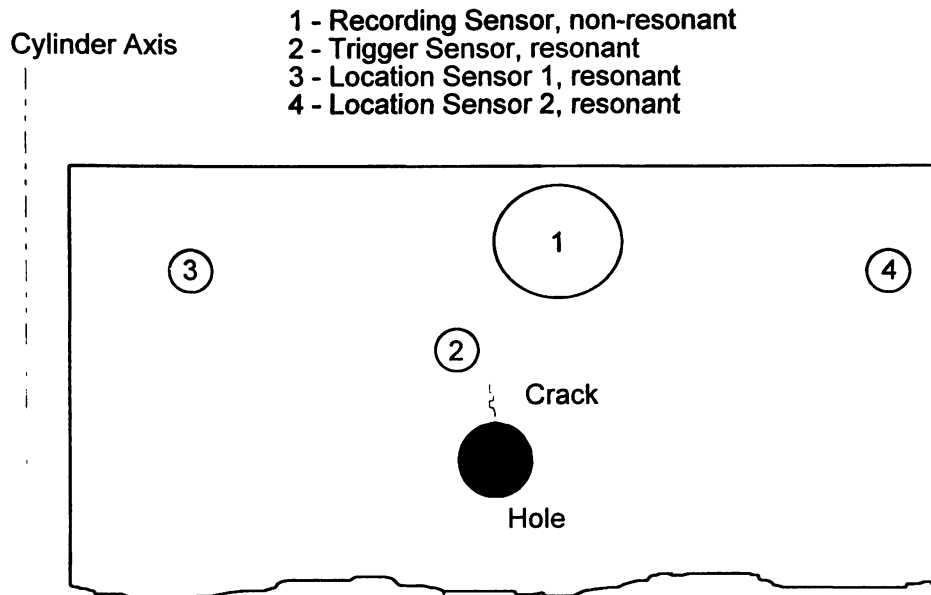


Figure 3.4 Placement of Acoustic Emission Sensor for Crack Signals

The placement of the trigger sensor was intended to minimize the possibility of noise signals being recorded. Each sensor was mounted on the pressure vessel using RTV, a black silicon sealant. It was thought that the most probable sources of noise signals would be located at the interfaces between the aluminum cylinder and the end plates. Attempts were therefore made to record noise signals from the endplates and at other positions on the vessel, but none of the noise signals had sufficient amplitude to cause the oscilloscope to trigger and record. These attempts at recording noise signals resulted in the establishing of a minimum threshold amplitude for triggering of the oscilloscope. Once the trigger level for the oscilloscope was determined, the sensors were then mounted at the positions shown in Figures 3.3 and 3.4 to conduct the desired tests.

In each instance, the trigger sensor was placed closest to the prospective AE

source, whether it was a line of rivets or a crack. This sensor would then be the first to detect the AE wave from a source. The trigger sensor monitored for the presence of an AE wave; its signal was then used to trigger the digital oscilloscope to record the raw AE waveforms from the non-resonant sensor. The other two resonant sensors were used for signal location, this being derived from the arrival times of the AE waves. All four of the sensors were connected to the LOCAN-AT. The trigger sensor and the recording sensor were also connected to the digital oscilloscope.

For rivet data collection, the location sensors and the recording sensor were placed parallel to the rivet line at the overlapping joint. The recording sensor was positioned on the surface of the vessel halfway between the two ends. The two location sensors were placed at least two inches from either side of the recording sensor. The trigger sensor was placed at least an inch closer to the rivet line than the recording sensor and an inch to one side of the recording sensor as shown in Figure 3.3.

For detection of cracks and rubbing, the sensors were placed close to the hole with the notch as shown in Figure 3.4. The positioning was varied to simulate signals coming from different places on the structure and to obtain a more comprehensive data set. Most of the signals recorded were found to originate from the same general area. The trigger sensor was placed closest to the point from which the AE waves were expected to propagate.

3.1.4 DATA ACQUISITION

The raw AE signals from the non-resonant recording sensor were captured and

displayed by the digital oscilloscope. The trigger level and the range on the oscilloscope were adjusted in the data acquisition program, NW1.BAS. The listing for this computer program is provided in the Appendix A. During a test, each waveform displayed on the oscilloscope was stored in a RAM drive in the 486DX2-50 computer as a data file. A RAM drive was used because of the speed at which data can be stored in the RAM drive is much greater than the speed at which data can be stored on a hard disk drive. The RAM drive was capable of storing 520 raw waveforms. Each test was therefore considered to be complete after the acquisition of 520 AE signals. When a test was completed, the files were transferred from the RAM drive to 3.5-inch, 1.44 MByte diskettes. After the data transfer was completed, the RAM drive was cleared, and the system was readied for the next test.

The signals from all four sensors were recorded by the LOCAN-AT. These signals were stored on the hard drive of the LOCAN-AT. The LOCAN-AT was used to power the sensors and to determine the location of the source of the AE waves recorded. A schematic of the data acquisition system is shown in Figure 3.5.

Provided that the energy of the signal measured by the trigger sensor was greater than the trigger level prescribed in the data acquisition program, the signals from the recording sensor were captured by the digital oscilloscope. The captured signals were displayed on the oscilloscope and transferred to the RAM drive of the 486DX2-50 computer. The data transfer was accomplished using an IEEE-488 card. For the maximum possible transfer rate, the format of the data was 8-bit (unsigned byte) data format, as opposed to the 16-bit format, which has higher resolution but a slower transfer

rate. As each wave was stored in the computer, they were tagged with a header at the beginning of the file that identified the vessel, the test number for the vessel, the time and date, the locations of the recording sensor and the trigger sensor, the trigger level of the oscilloscope, the range and time base for the oscilloscope, the pressure level when the wave was recorded, the cycle number referenced to the beginning of the test, and the part numbers for the sensors. The pressure readings were gathered from the pressure transducer connected to the vessel and measured using a digital voltmeter that transferred the pressure data to the computer.

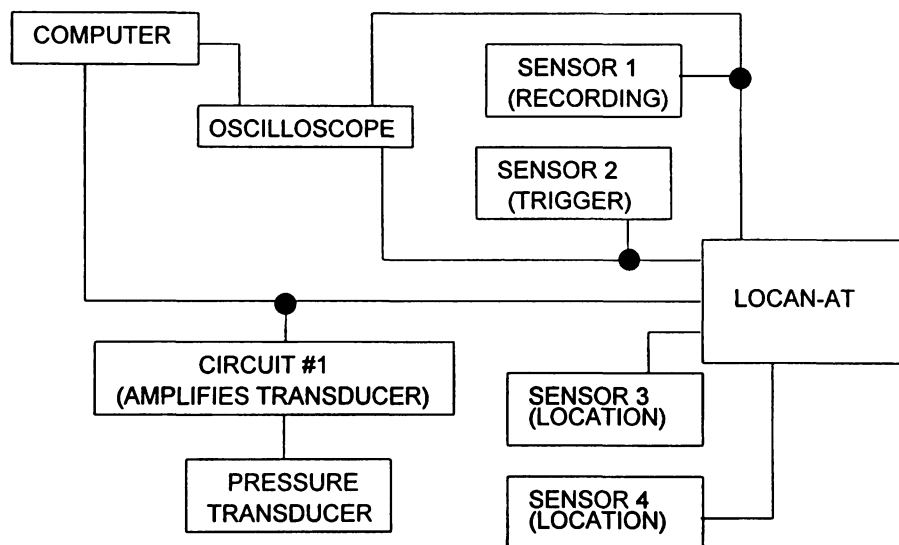


Figure 3.5 Instrumentation Configuration

3.2 DATA CONDITIONING

3.2.1 PREPROCESSING

After the data was collected, the raw signal files were preprocessed for later use in the neural network. The preprocessing of the data was accomplished in five steps: (1) AE

signals were recorded as binary files, (2) converting binary files into ASCII files, (3) eliminating noise signals by requiring the AE signal to have a minimum amplitude, (4) determining the power spectrum for each AE signal, and (5) linearly reducing the number of points which represent the power spectrum from 800 to 67. The reduction from 800 to 67 data points was determined through optimization of the neural network. If more than 67 points were used as input data for the neural network, the resolution of the results was not greatly enhanced yet the training time for the network was greatly increased.

The recording of the signals as binary files was accomplished through the use of the digital oscilloscope and the computer. The elimination of the low amplitude signals involved the use of a basic program called NOISE.BAS (Appendix B). The threshold amplitude chosen for elimination of the noise signals was 18 millivolts, which was 3 millivolts above the noise level of the system during operation. The determination of the power spectra for all of the remaining signals was conducted using a software package called DADiSP. DADiSP took the raw signals, found the power spectra, and then linearly reduced the number of points representing the spectra. The data acquired by the LOCAN-AT were used to verify the location and source of the signals obtained. Figure 3.6 shows a time based AE signal of 200 μ s in length as recorded by the digital oscilloscope.

The signal from the AE sensor was digitized by the oscilloscope and then transferred to the computer. The power spectrum for the digitized AE signal was determined using a Fast Fourier Transform (FFT) function provided by DADiSP. Figure

3.7 shows an example of a linearly reduced power spectrum as determined by the DADiSP software program.

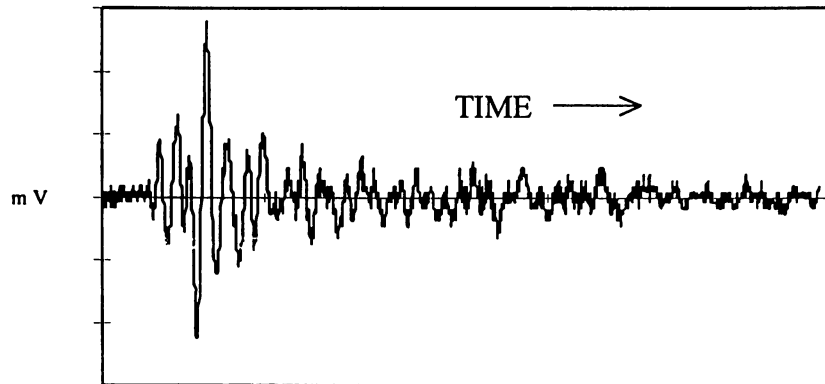


Figure 3.6 Digitized AE Signal

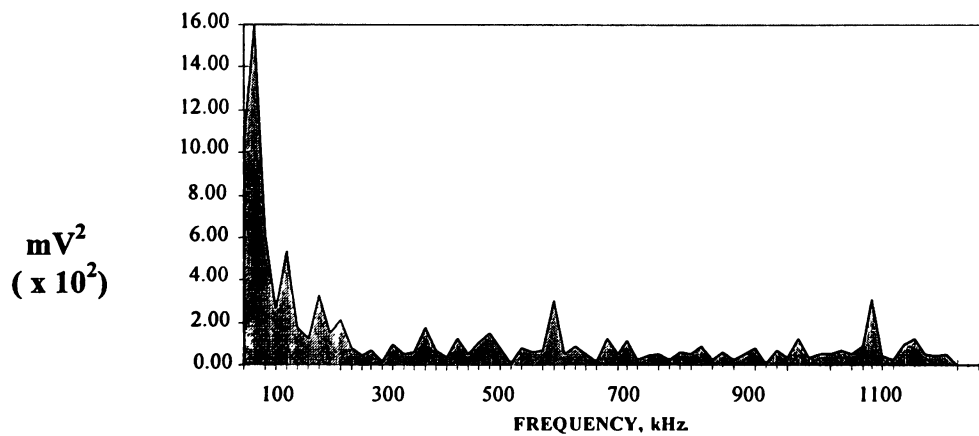


Figure 3.7 Linearly Reduced Power Spectrum

3.2.2 BANDWIDTH REQUIREMENTS

As previously stated, the recording sensor was a non-resonant (wide band) type sensor with a response bandwidth from 100 kHz to 1.2 MHz. The signal recorded is typically very close to the true signal because the majority of source mechanisms generate AE waves that are composed of frequencies within the bandwidth of the sensor

used. Some harmonics of frequencies could be higher than the sensor can measure, but the amplitude of those frequencies would be much less than the amplitude of the fundamental frequencies due to attenuation. The high end limit of the wide band sensor is one of the controlling factors for the selection of the sampling rate for the digital oscilloscope. The sampling rate must be such that aliasing of the AE signal will not occur. An example of aliasing is given in Figure 3.8, where the solid line indicates the real signal and the dashed line the aliased representation of that signal.

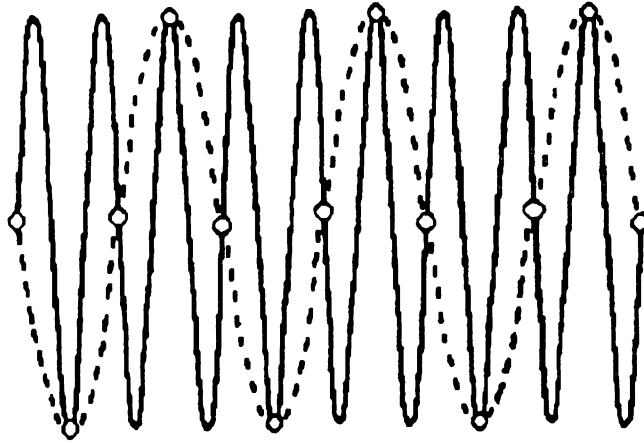


Figure 3.8 Aliasing of Signal Due to Improper Digital Sampling Rate

The possibility of aliasing was the critical factor for choosing 8-bit data format rather than 16-bit data format. The 16-bit data format would require twice as long for transfer from the oscilloscope to the computer. When the sampling rate is too slow, signals are incorrectly perceived or aliased as seen above. This can be avoided by keeping the sampling rate on the order of ten times greater than the highest frequency of the signal to be measured. Therefore, a sampling rate of 10 MHz was chosen for this research. Because of limits imposed by the oscilloscope, a 10 MHz sampling rate meant

that the resultant waveform was 200 microseconds in length. It was thought that while most AE events could be measured within that time interval, combined signals such as rubbing plus cracking might last longer than 200 microseconds; however, no combined signals were encountered.

3.3 TESTING PROCEDURE

Conducting each test run consisted of clearing the RAM drive, starting the pressurization system, initializing the computer and digital oscilloscope, running the data acquisition program on the LOCAN-AT, acquiring 520 AE signals, stopping the pressurization system, transferring data files, and checking for air in the system, which, if present, was then bled off (Figure 3.9). A total of eighteen runs were performed on the pressure vessel. The tests produced three general categories of AE activity -- cracks, rivet fretting, and rubbing -- plus some extraneous noise.

The three general classifications were determined initially by the sensor placement and the expected AE sources to be monitored. Each general classification was broken down into two subsets. One subset included the data collected while pressurizing the vessel from 20 to 80 psi at a rate of 1 Hz. The second subset was the data collected while pressurizing the vessel from 20 to 80 psi at a rate of 0.5 Hz. Two different rates for pressurization were used in order to obtain a more comprehensive data set, in that a practical application would not necessarily be restricted to one frequency during operation. Changing the recording sensor position was performed at random in order to further the diversity in the data.

After three tests were performed for each pressurization frequency, the sensors were moved to the next location where the next AE source was expected to occur. The rivet line was the location for the first series of tests. After rivet fretting signals were recorded from the rivet line, the sensors were moved to the area on the vessel close to the circular cutout. Rubbing signals were then obtained. At the same time the notched area was monitored to determine the onset of crack growth. This monitoring consisted of unaided visual inspection. When a crack was verified through visual inspection, the sensors were moved a small distance, and recording of crack signals commenced.

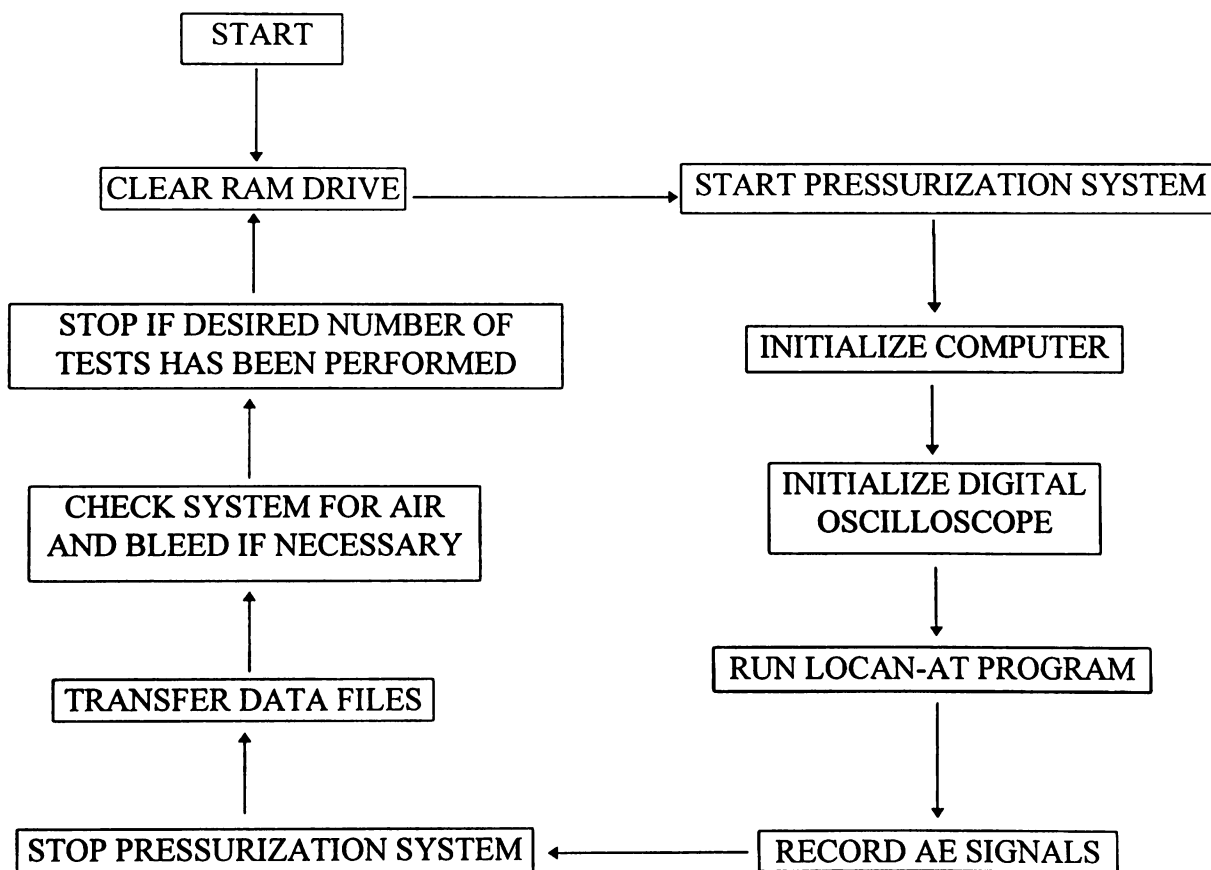


Figure 3.9 Testing Procedure

CHAPTER 4

NEURAL NETWORK ARCHITECTURE, OPERATION, AND IMPLEMENTATION

4.1 SELECTION OF A NEURAL NETWORK

4.1.1 INPUT DATA FOR THE NEURAL NETWORK

The input data sets for the neural network were the power spectra of the AE signals that were recorded during testing of the pressure vessel. Each power spectrum consisted of 67 numbers whose values ranged between -1 and 1. Figures 4.1, 4.2, and 4.3 show the power spectra for a rivet signal, a rubbing signal, and a crack growth signal. While the power spectra shown were chosen as examples to show the differences between the three source mechanisms, the differences in many of the spectra were much more subtle.

Generally speaking, if patterns in the data are discernible to the naked eye, a neural network can be trained to classify them. A first pass through the data yielded approximately 15 different patterns; and over 23 different patterns resulted from a second evaluation; whereas only 4 patterns were expected, one each for rivet fretting, rubbing and crack growth plus a final category for noise. From this it became evident that the information contained in the power spectra was too detailed to allow good *visual* discrimination between the various source mechanisms.

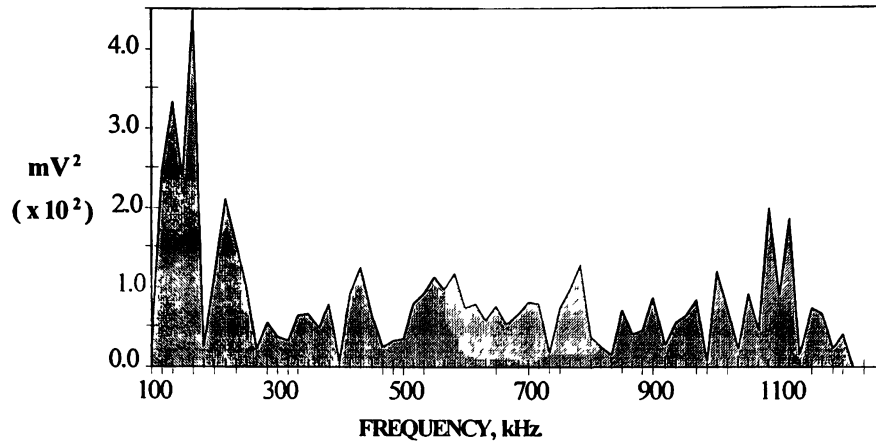


Figure 4.1 Rivet Signal Power Spectrum

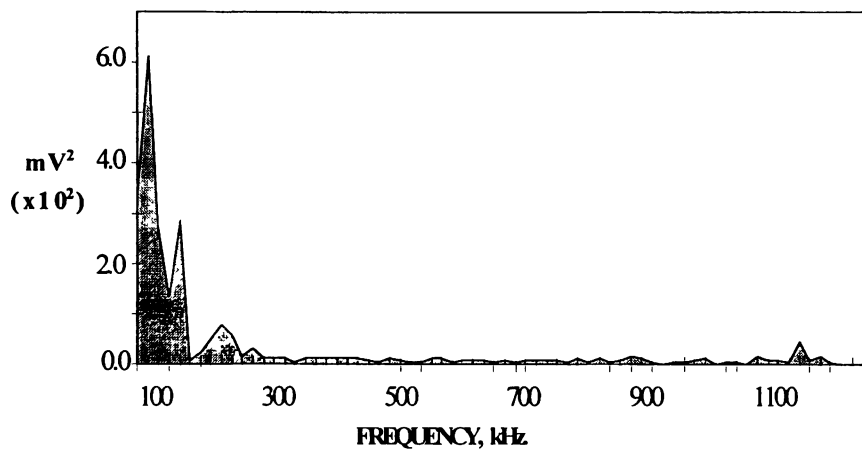


Figure 4.2 Rubbing Signal Power Spectrum

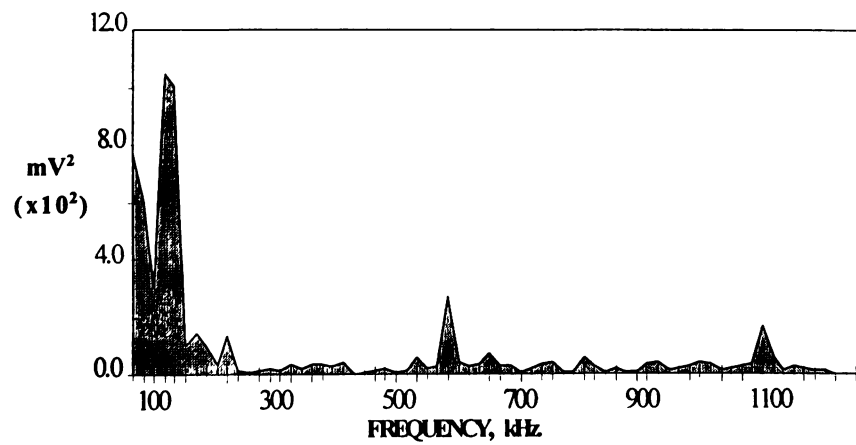


Figure 4.3 Crack Signal Power Spectrum

In Figure 4.4, two rivet signal power spectra are shown. A vast majority of the rivet signals were similar but still possessed enough variation to make classification difficult. The reason for this was that there were many different possible sources for the rivet signals. To reduce the amount of detail contained in the input data, it was necessary to review the time-based AE signals.

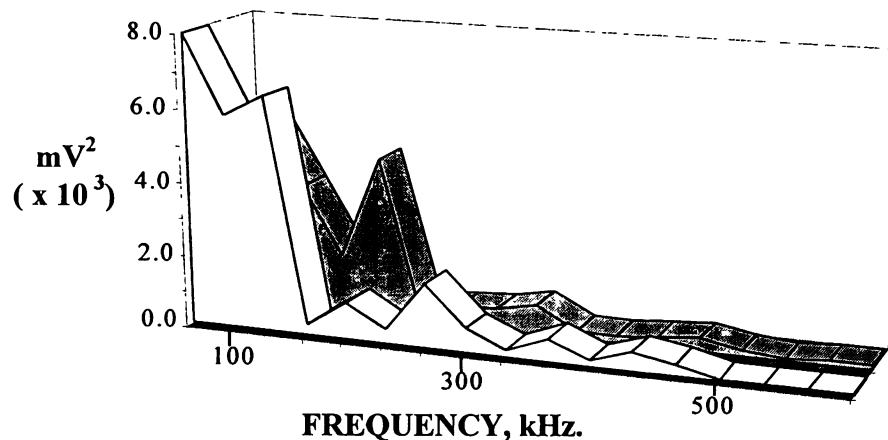


Figure 4.4 Two Rivet Signals With Different Power Spectra

4.1.2 JUSTIFICATION FOR USING A NEURAL NETWORK

Visual inspection of recorded AE signals resulted in the recognition of patterns that were consistent with the different types of AE signals (Figures 4.5, 4.6, and 4.7). The dashed lines in Figures 4.5, 4.6, and 4.7 represent voltage threshold levels. The threshold levels were all set at 18 millivolts, which was 3 millivolts higher than the background noise. The threshold level is used to show the difference in duration of the signals. The total length of each x-axis for the figures represents 200 microseconds. The duration of each signal is determined as the time from when the signal first exceeds the threshold until it falls below the threshold for at least 50 microseconds.

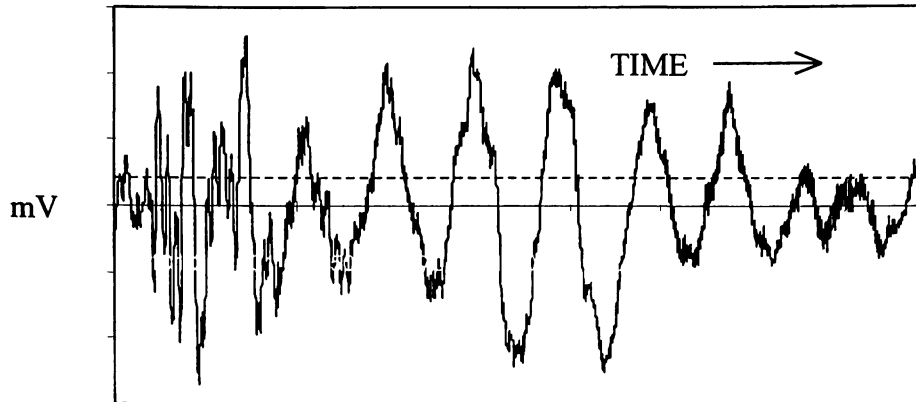


Figure 4.5 Recorded Rivet AE signal

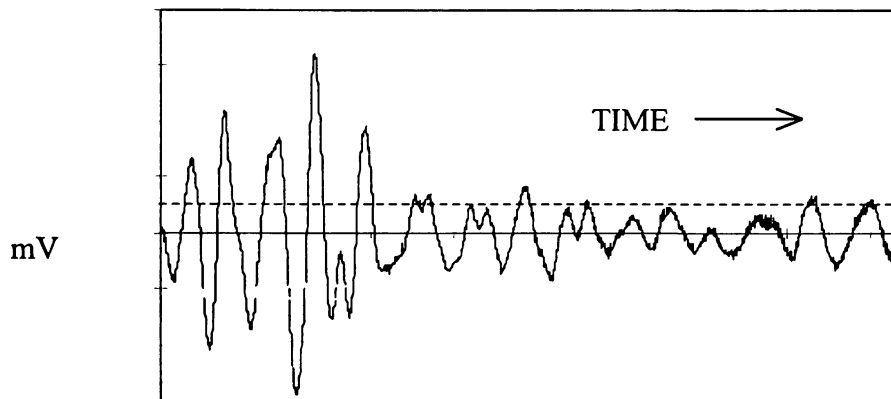


Figure 4.6 Recorded Rubbing AE Signal

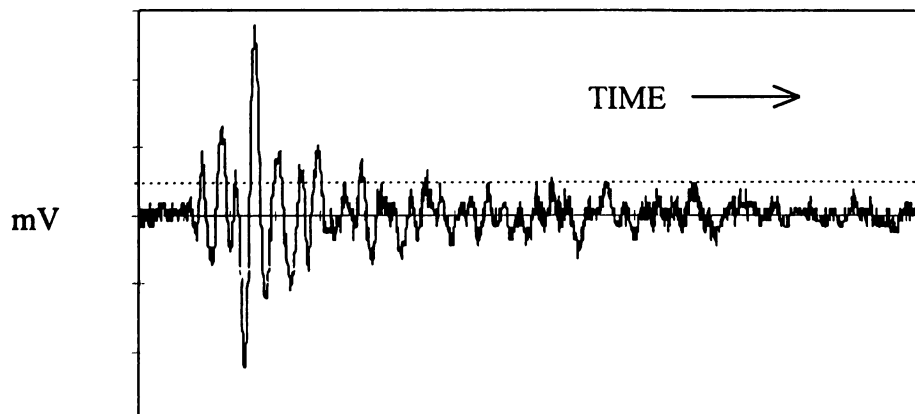


Figure 4.7 Recorded Crack AE Signal

From this it was estimated that the crack signal had a duration of approximately 40 microseconds and that the durations for the rivet signal and the rubbing signals were 180 and 100 microseconds, respectively.

Even though patterns were visually evident, the recorded AE signals were not used as input data sets because the digitized waveforms, consisting of 2,000 data points, would need to be used as input to the network. If these raw waveforms were used, the network would require an excessive amount of training time because of the large number of data points. The training time for a network is related to the square of the number of data points for each input. The power spectra, on the other hand, provide the salient features of the raw waveforms while requiring fewer data points for accurate representation. Hence, the power spectra were used as network input rather than the raw waveforms. After determining the feasibility of a neural network and the appropriate input data, the next step was to select the specific neural network.

4.2 ARCHITECTURE OF NEURAL NETWORK SELECTED

There are a number of classification networks available within the *Neural Networks Professional II / PLUS* software package so the selection criteria were narrowed. Without a lengthy and in-depth manual analysis of the more than 5,000 waveforms involved, a network requiring supervised learning was not thought to be practical. Thus, the choice for a network was restricted to all those capable of classification using unsupervised learning. The only network available that met the selection criteria was a self-organizing map (SOM).

A SOM is a neural network that typically consists of three layers. The three layers are an input layer, a processing layer, and an output layer. Figure 4.8 illustrates the SOM general architecture with the input neurons fully connected to each one of the processing elements (PEs) in the middle or hidden layer. Each PE in the hidden layer is connected to the output neurons and is fully interconnected to the other neurons in the hidden layer. The hidden layer is also known as the Kohonen layer, named after Tuevo Kohonen who developed the SOM. The hidden layer is considered to be a two-dimensional layer as shown in Figure 4.8.

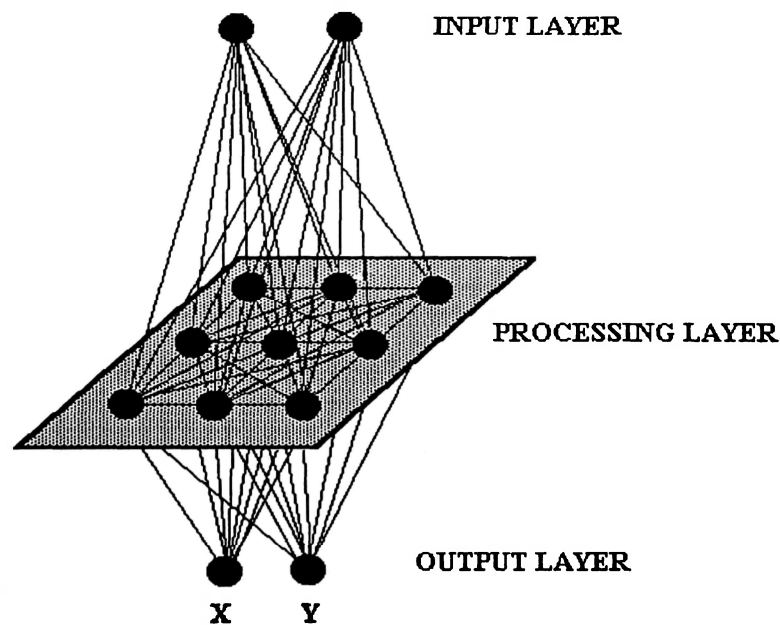


Figure 4.8 Self-Organizing Map General Architecture

The capability of the SOM to accurately classify data is dependent on the number of processing elements. Although there is not a given method for determining the

optimum number of PEs in the hidden layer, the number of inputs is related to number of processing elements. The larger the number of inputs, the larger the number of PEs required in the hidden layer. Also, the greater the complexity of the data, the larger the number of PEs required.

The SOM classifies data with similar characteristics into groups. The actual numerical output for the SOM is in the form of x and y coordinates which are then put into a supplemental program to plot the results. The final output is a two-dimensional topological map that depicts different classifications of data sets as different clusters of points. An example of a SOM with three categories or classes is shown in Figure 4.9.

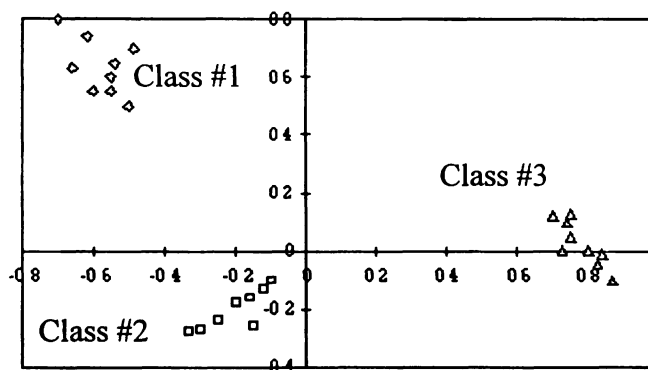


Figure 4.9 Example of a SOM With Three Classes

As mentioned earlier, the SOM is capable of providing topological representations of complex data, but the parameters for the network must be chosen properly, and the data must be separable in some manner. If the signals are indistinguishable by visual inspection, application of any type of neural network would be unpredictable. For the purpose of this research, it was shown that there is a discernible difference between the power spectra for the AE signals generated by the different AE sources.

4.3 NEURAL NETWORK OPERATION

The hidden layer is the layer that allows the SOM to complete its task. All of the processing elements in the hidden layer are fully interconnected with each other, and the interaction between the PEs is considered to be a competition. The Euclidean distance of each PE is calculated, and the one with the smallest Euclidean distance is the winner.

The Euclidean distance measures how much of a difference there is between the signal desired by the PE and the actual incoming signal. The Euclidean distance is defined as

$$D = \|X - W\| = \sqrt{\sum_{i=1}^n (x_i - w_i)^2}$$

where n is the number of input values, X is the set containing the input values, and W is the set containing the corresponding weight values:

$$X = (x_1, x_2, x_3, x_4, \dots, x_{67})$$

$$W = (w_1, w_2, w_3, w_4, \dots, w_{67}).$$

The value for n was 67. The number of inputs was chosen after a series of tests were performed on the network, and it was determined that 67 inputs was optimum. Here the number of inputs was the number of data points representing the power spectrum for each waveform. Increasing the number of inputs did not significantly influence the SOM results but greatly increased the training and processing time for the network. The number of inputs investigated were 50, 67, 75, and 100. With each input data set there is a winning PE, which is, in a measurable way, the closest to the input value and thus represents the input value. The winning processing element has an output, while the

losing PEs do not. The output of the winning PE is translated into a coordinate by the output neurons. These resulting coordinates represent the input signal to the topological map.

After a winner has emerged, the processing elements in the immediate vicinity (neighborhood) of the winner adjust their weights to more closely resemble the winning PE. This process allows for finer discrimination of the input data. Once the network has been trained, the weights for all of the neurons are held constant. As the network is being trained, there is a change in the actual size of the neighborhood around the winning PEs. If the losing PEs were allowed to change for the entire training period, the result could be a network that does not learn to classify the input data. The size of the neighborhood is decreased incrementally while the net is being trained. The final neighborhood size is chosen to be either 1 or 2 as shown in Figure 4.12.

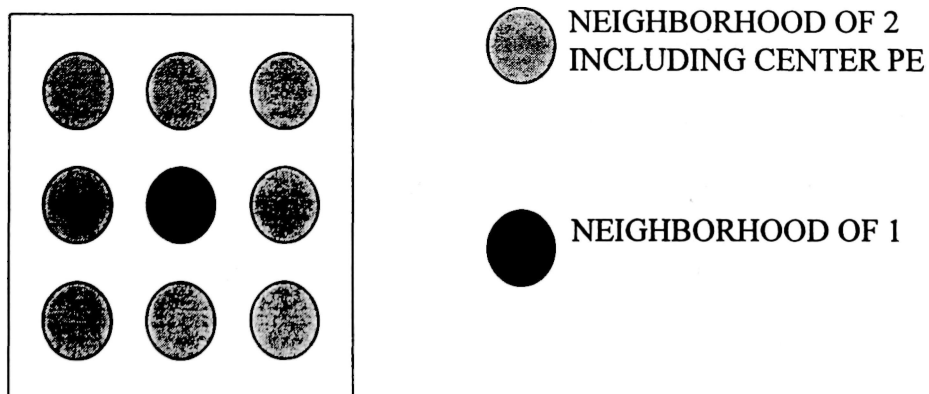


Figure 4.12 Neighborhood of a Self-Organizing Map

The training parameters control the changes that occur in the hidden layer during the training of the network. The six parameters that control the changes to the network

are (1) the learning coefficient (α), (2) the learning coefficient ratio, (3) beta (β), (4) gamma (γ), (5) the transition point, and (6) the number of SOM steps. The learning coefficient is a number that aids the iterative process of changing the weights for the network connections. The learning coefficient effects are described by the equation

$$(w_{ij})_{\text{new}} = (w_{ij})_{\text{old}} + \alpha[x_j - (w_{ij})_{\text{old}}]$$

where the terms w_{ij} are the values for the weights of the neurons, and α is the learning coefficient.

The learning coefficient ratio is the multiplier used to reduce the learning coefficient after the transition point is reached. The learning coefficient is reduced so that the change in weights becomes less and less as the network trains. Without this feature, the values for the output of the network can sometimes oscillate between two numbers and never home in on the desired answer. The learning coefficient ratio is applied to the learning coefficient at the operator specified transition point.

The transition point is the number of SOM steps that must occur before the changes to the weights will be made. The transition point should be at least equal to the number of training data sets, if the data represents a complex system, and if the system is extremely complex, the transition point is typically set to be twice the number training data sets. The number of SOM steps is the total number of iterations that the network will train. One iteration is the processing of one input data set.

The remaining two parameters, beta(β) and gamma(γ), control the frequency at which a processing element is allowed to win. The controlling or conscience mechanism

keeps track of how often a PE wins and adjusts the network to encourage the losing processing elements to win more often. This allows better separation of the categories on the output map. The gamma(γ) is used to adjust a bias which increases the Euclidean distance for the winning PE, thus making the losing neurons more competitive. The bias term (B_i) is computed as

$$B_i = \gamma(N \cdot F_i - 1) \quad i = (1, 2, 3, 4, \dots, 67)$$

where N is the total number of processing elements in the hidden layer, i is the number of input neurons, and F_i is the frequency of how often a specific neuron has won. As the network trains, the bias term affecting the Euclidean distances needs to become less or the network may never become fully trained. The value for the frequency term is updated at each transition point and is modified by the beta (β) parameter. The frequency for the winning PE is modified by the equation

$$F_i = (F_i)_{old} + \beta[1-(F_i)_{old}].$$

The frequency term for all losing neurons is changed by the equation

$$F_i = (F_i)_{old} - \beta(F_i)_{old}.$$

The complexity of neural networks does not encourage any detailed rules for the determination of these six control parameters. There are general guidelines for selecting the parameters, but these guidelines vary with the complexity of the input data. For this research, the parameters were determined through trial and error.

4.4 NEURAL NETWORK IMPLEMENTATION

The SOM used for this research was contained in the *Neural Networks Professional II / PLUS* software package. To construct a SOM, a utility called *Instanet* was used. The operator specified inputs for the *Instanet* utility were the controlling parameters, the number of inputs, the number of processing elements in the hidden layer, and the number of output neurons. These were all entered into the program. The number of output neurons was automatically set at two if the mapping network option was selected. In the software package, a SOM is considered to be a front end processor for another neural network if the *coordinate layer* option is not selected. The number of input neurons was set to 67, and the first choice for the number of PEs in the hidden layer was 900. Once the controlling parameters were determined, three other networks were trained using the same control parameters. The other three networks used 225, 400, and 1225 PEs in the hidden layer.

4.4.1 SELECTION OF CONTROLLING PARAMETERS

The six control parameters for the trained SOM are listed in Table 4.1. These parameters were determined through trial and error. The process involved iteratively training and testing a network. The training of each of the networks used the same exact training file. The testing file was also the same for each network, but the contents of the test file were generally known. The LOCAN-AT was used to determine the location of most of the sources for the recorded AE signals and thus allowed a preliminary

classification of the signals for the test file. The output of the network was then imported into *Microsoft Excel 5.0*, and a two-dimensional plot was generated. A printout of the plot was obtained, and then a new network was made. Each new network was created by varying one control parameter at a time. This process was used to develop the network most capable of classifying the input data. The printouts of the results from testing the networks were compared to determine which had the best clustering and the least amount of overlap between the clusters.

# SOM Steps	101,340
Beta (β)	0.3
Gamma (γ)	0.01
Learning Coefficient	0.5
Learning Coefficient Ratio	0.4
Transition Point	10,032

Table 4.1 SOM Control Parameters

Other parameters that were selected for the SOM are presented in Table 4.2. The selection to *interpolate* the output allowed the network to interpolate a coordinate from the three top winning processing elements. This function increased the resolution for the SOM. The selection of *coordinate* for the output layer enabled the SOM to have a two-dimensional map as an output. For the neighborhood starting width, a value of 8 was chosen according to the recommendation in the software users manual, and for the ending width, a value of 1 was chosen for the same reason. The shape of the neighborhood was

chosen to be square. No information was given as to the benefits of selecting a diamond shape for the neighborhood.

Number of Inputs	67
Number of Processing Elements in Hidden Layer	30 x 30 (total of 900)
Output Layer	Coordinate
Output Processing Function	Interpolate
Neighborhood Starting Width	8
Neighborhood Ending Width	1
Neighborhood Shape	Square

Table 4.2 SOM Architecture and Processing Parameters

4.4.2 TRAINING THE NEURAL NETWORK

During testing of the pressure vessel, a total of eighteen sets of data were gathered, six sets for each prospective source mechanism. Each set consisted of approximately 520 acoustic emission raw waveforms. After the processing of the data was completed, there were 5,500 power spectra remaining. For each anticipated source mechanism, four data sets were selected at random (from the six sets) to be used to train the network.

A total of twelve separate data sets were combined into one file to simplify the training process. The training file consisted of 3,600 power spectra. To begin training of the network, the control parameters were set, and then inputs were selected at random (by the program) from the training file. The entire training file was processed through the network a total of thirty times. After training, the network was tested to determine if the data were being classified properly.

4.4.3 TESTING THE NEURAL NETWORK

With two thirds of the processed data being used for training, the remaining third was used for testing the network. The test data were sorted into three separate files according to what the most likely source mechanism had been recorded. The prospective source mechanism was determined by the location of the recording sensor and the trigger sensor. One training file consisted of primarily crack growth signals, another consisted of primarily metal on metal rubbing signals, and the third set consisted mainly of rivet fretting signals.

Each test file was processed once through the trained network. The three output files from the network were transferred to *Microsoft Excel 5.0* which generated the two-dimensional topographical map. For each output file, a different symbol was used to allow easier visual inspection of the results. If the test sets had not been segregated and different symbols were not used to represent the different testing sets, the resulting topological map would have been very difficult to interpret.

CHAPTER 5

ANALYSIS AND VERIFICATION OF RESULTS

The results from this research are summarized in two-dimensional topological maps. These plots depict similar input data as clusters of points on an x-y plot. The SOM plots presented show a progressive improvement in the classification ability of the neural networks trained from the initial network, which was able to partially classify the input data, to the final network that was able to fully classify the data.

5.1 PRELIMINARY NETWORKS AND THEIR RESULTS

The SOM results shown below were generated from networks trained with varying control parameters. Early experimentation found that varying the learning coefficient, the learning coefficient ratio, and the number of SOM steps did not have a large effect on the network output. The parameters controlling the frequency at which a PE can win, beta (β), and the bias term associated with that PE, gamma (γ), were found to have a large effect on the classification performance of the networks. With each result plot shown, the values beta (β) and gamma (γ) are given.

The SOM shown in Figure 5.1 was generated by one of the first networks trained. It is apparent, from visual inspection that the network was unable to completely sort the input data as desired. The amount of overlap between the clusters shows that the

neural network was only partially classifying the input data. A properly trained network may have overlap, but it would not be nearly as pronounced as that in Figure 5.1.

The change in the gamma (γ) between SOM #1 and SOM #2 reduced the overlap between the data clusters (Figure 5.2). Here the beta (β) value was held constant to determine the effect of reducing gamma (γ). All other control parameters were held constant.

Numerous iterations consisting of varying the beta (β) and the gamma (γ) parameters resulted in a SOM with a minimum of overlap. The other parameters were then varied but had very little effect on the resulting SOM. This optimized classification output is shown in Figure 5.3. The control parameters for this final SOM are listed in Tables 4.1 and 4.2. Notice that there is some overlap between the clusters of the data; therefore, further analysis was pursued to determine the cause.

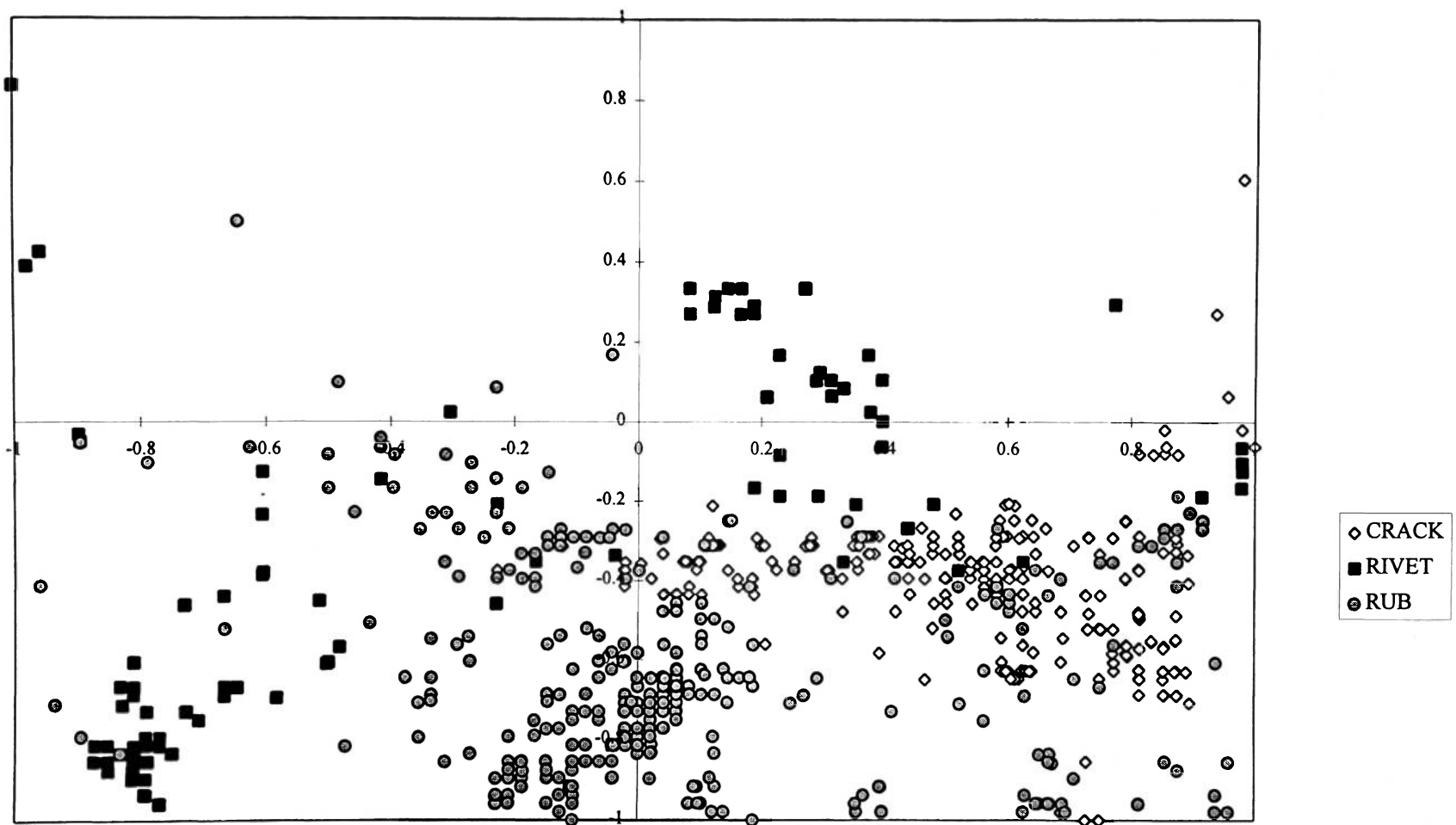


Figure 5.1 Preliminary SOM #1, $\beta = 0.0003$, $\gamma = 0.9$

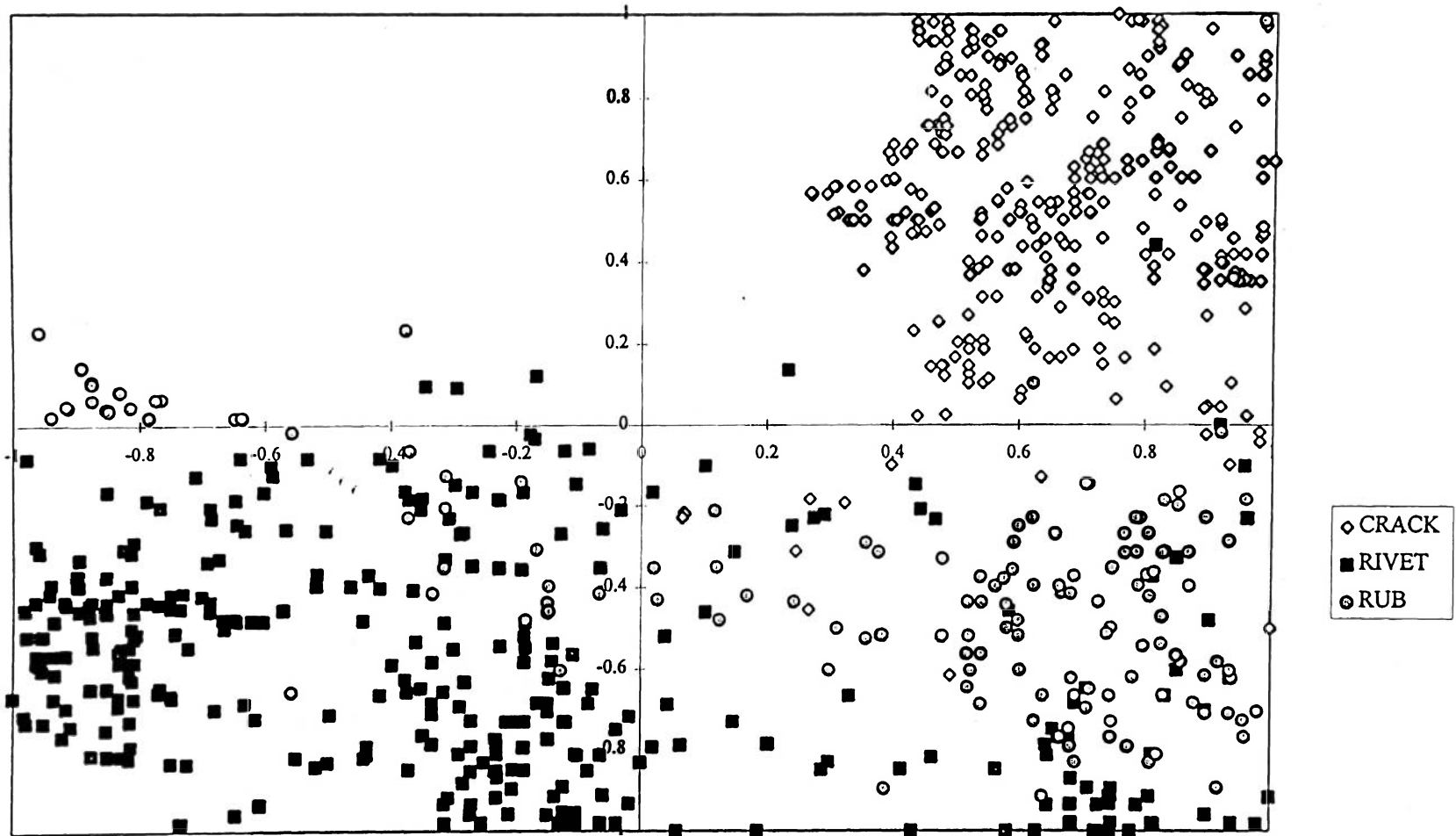


Figure 5.2 Preliminary SOM #2, $\beta = 0.030$, $\gamma = 0.5$

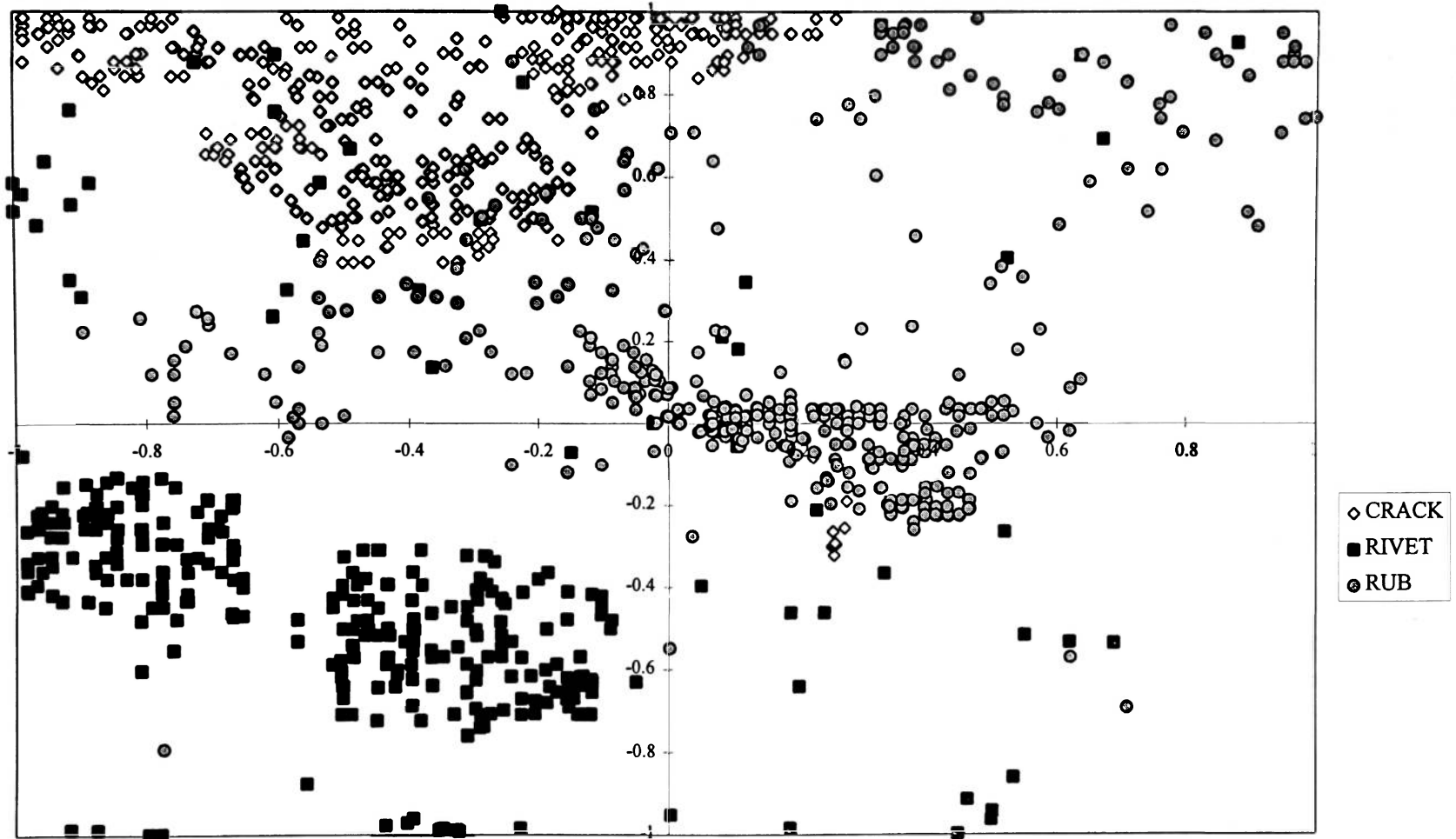


Figure 5.3 Final SOM, beta = 0.3, gamma = 0.01

5.2 ANALYSIS AND VERIFICATION OF RESULTS

The preliminary classification of the AE signals consisted of identifying the expected source and grouping the signals accordingly. If the sensors were placed close to the two rivet lines, then the signals collected were classified as rivet fretting. The same applied to the crack signals and the rubbing signals. The rubbing signals were not expected to contain crack signals because visual inspection did not detect any cracks. This point by point analysis of the signals resulted in a new SOM corrected for improper initial classification.

The point by point analysis consisted of six steps.

1. Location of the points in the distinct groups were determined using the LOCAN-AT.
2. Location of the points in the overlap areas were determined using the LOCAN-AT.
3. The mechanism for each point was extrapolated from the location of the signal.
4. The power spectra for the points with known mechanisms and those without were compared.
5. Those points with erroneous initial classifications were reclassified.
6. Results were plotted after the overlap areas were analyzed.

The location was used for the extrapolation of the mechanisms. For example, if the location of the AE signal was found to be at the position of a rivet then the signal was reclassified as a rivet signal. The points with known mechanisms were clustered into regions. These regions are shown in Figure 5.4. The region of primary concern was that which contained the crack signals.

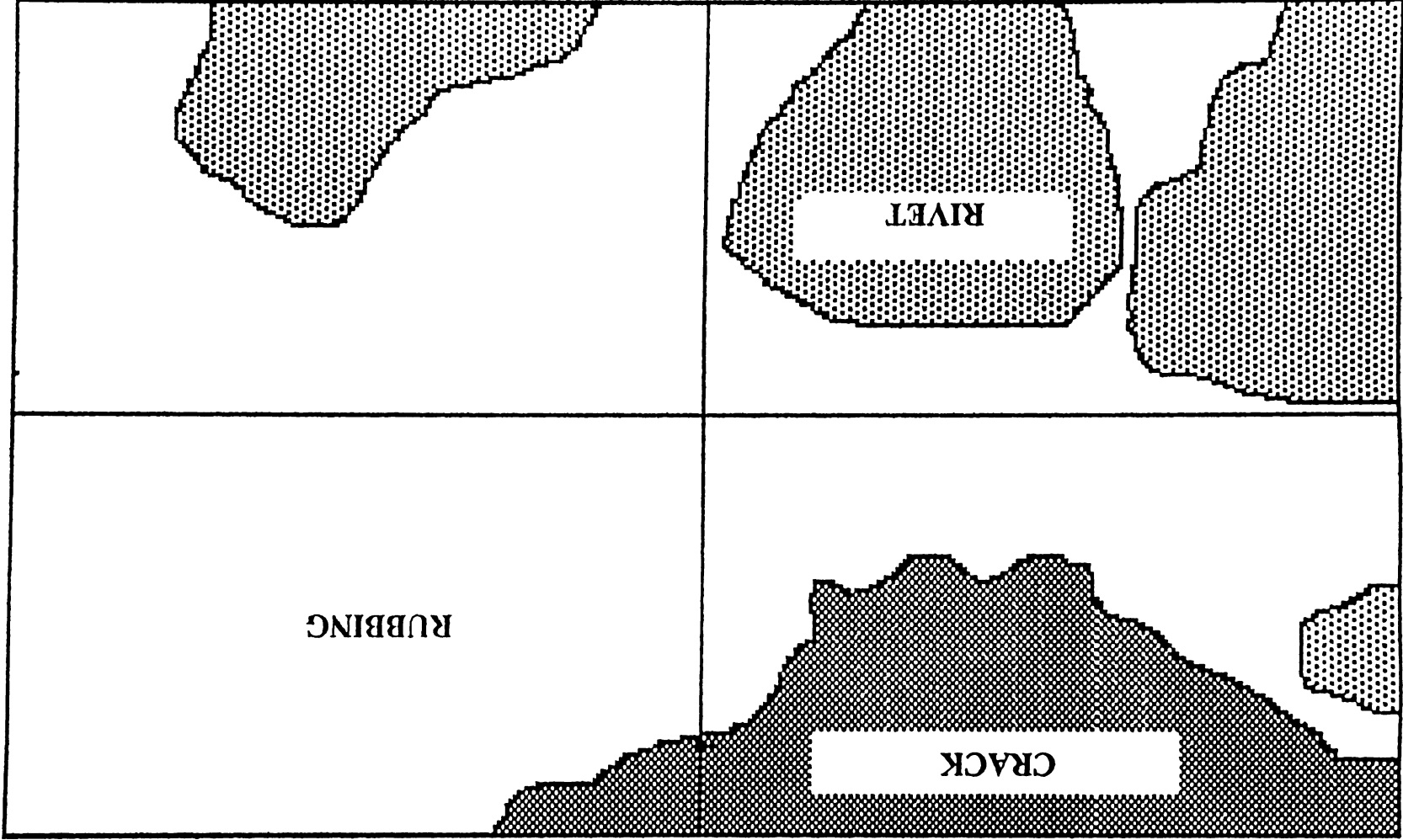


Figure 5.4 General Regions for Mechanisms as Classified by the Final SOM

Finally, the SOM plotted with the signals corrected for initial misclassification is shown in Figure 5.5. Here the overlap between the regions was eliminated such that classification of the signals according to mechanism (rivet, rubbing, or crack) was complete. At this point the SOM was trained and ready for real-time implementation.

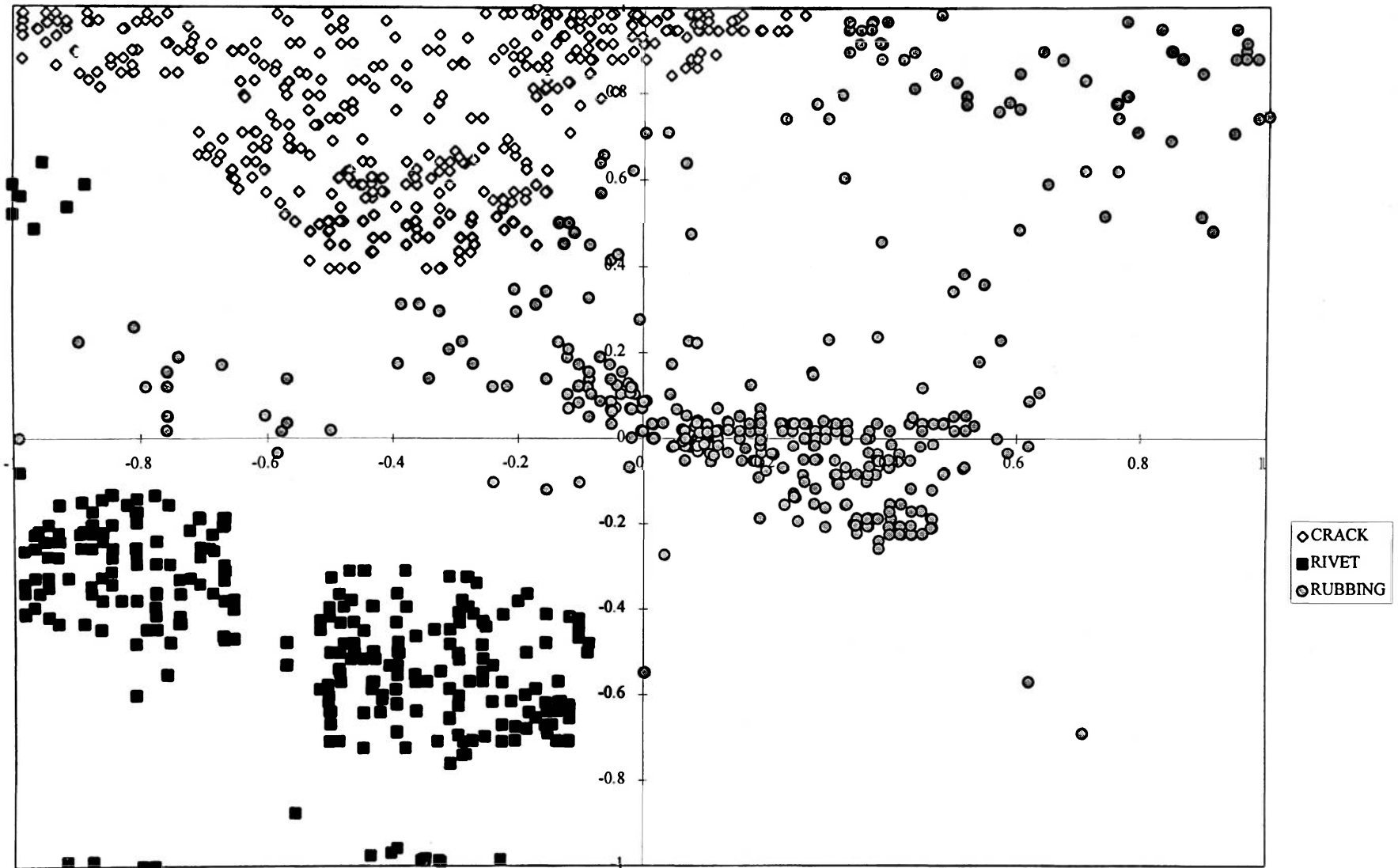


Figure 5.5 Final SOM for Corrected Data

CHAPTER 6

CONCLUSIONS AND RECOMMENDATIONS

6.1 CONCLUSIONS

- Acoustic emission nondestructive testing can be used to monitor fatigue crack initiation and growth in complex structures made of thin aluminum.
- A self-organizing map neural network was proven to be capable of classifying source mechanisms from 67 point power spectra taken from acoustic emission waveforms sampled at 10 MHz.
- All overlap in classification clusters was found to be the result of operator misclassification, e.g., crack signals that originated from areas where rivet fretting was the predominant mechanism, etc..

6.2 RECOMMENDATIONS

Subsequent to acoustic emission testing of the 2024-T3 aluminum pressure vessel used in this research another 2024-T3 aluminum pressure vessel plus three 7075-T6 aluminum pressure vessels were tested. It is recommended that data gathered be used to train another network to classify source mechanisms on all five vessels at once. Another

extension of this research would be to train a network to classify source mechanisms using the acoustic emission (AE) parameter data provided by the LOCAN-AT and compare the results to this research. This would allow a comparison between the classifications provided by the waveform analysis and the AE parameters . Further iterations could also be performed on the final SOM network to determine if a better (smaller and more distinct clustering) network could be generated. Finally, other classification networks such as Adaptive Resonance Theory 2 (ART2), Linear Vector Quantization (LVQ), and Probabilistic Neural Network (PNN) could be investigated.

REFERENCES

1. O'Lone, R.G., "Safety of Aging Aircraft Undergoes Reassessment," Aviation Week and Space Technology, Vol. 128, Issue 20, May 16, 1988, pp. 16-18.
2. McBride, S.L., and Maclachlan, J.W., "Acoustic Emission Due to Crack Growth, Crack Face Rubbing, and Structural Noise in CC-130 Hercules Aircraft," Journal of Acoustic Emission 3 (April 1984), pp. 1-9.
3. Parish, B.S., "An In-Flight Acoustic Crack Detection System (ACDS) for the C/KC-135 Aircraft," Presented at the National Fall Conference of the American Society for Nondestructive Testing, Columbus, Ohio, October 1979, pp. 33-35.
4. Rodgers, J., "Acoustic Emission in Aircraft Structural Integrity and Maintenance Programs," Journal of Acoustic Emission 1 (April 1982), pp. 113-120.
5. Prosser, W.H., Aerospace Technologist, Nondestructive Evaluation Science Branch, NASA Langley Research Center, Hampton, VA.
6. Hill, E., Walker, J.L., and Rowell, G.H., "Burst Pressure Prediction in Graphite-Epoxy Pressure Vessels Using Neural Networks and Acoustic Emission Amplitude Data," submitted for publication to Materials Evaluation January 1995.
7. Hill, E.v.K., Israel, P.L., and Knotts, G.L., "Neural Network Prediction of Aluminum-Lithium Weld Strengths from Acoustic Emission Amplitude Data," Materials Evaluation, Vol. 51, No. 9, 1993, pp. 1040-1045, 1051
8. Ely, T.M., and Hill, E.v.K., "Neural Network Classification of Acoustic Emission Data from Graphite/Epoxy Tensile Test Specimen," presented at National Spring Conference of the American Society for Nondestructive Testing, Las Vegas, Nevada, April, 1995, pp. 109-111.

BIBLIOGRAPHY

1. Fausett, L., Fundamentals of Neural Networks, Architecture, Algorithms, and Applications, (Englewood Cliffs, N.J.,1994).
2. Neural Computing: NeuralWorks Professional II/PLUS and Neuralworks Explorer (NeuralWare, Inc. Technical Publications Group, 1991).
3. Miller, R. K. and McIntire, P., Acoustic Emission Testing, Volume 5 of Nondestructive Testing Handbook, second edition (Columbus, Ohio.: American Society for Nondestructive Testing, 1987), 115.

APPENDICES

APPENDIX A
NW1.BAS, BASIC COMPUTER PROGRAM

'This program uses a IEEE-488 to interface a Kiethley 197 DMM and a
 'HP 54601a digital oscilloscope to a IBM 486 computer. The program
 'will acquire acoustic emission waveform data near the point of
 'maximum load during fatigue cycling and store them on a RAM disk.

'Program written by Glenn Greiner Summer 1993 and
 'modified by Paul Thornton Summer A 1994

```
OPTION BASE 1
DIM wave$(10000)
INPUT "Enter the Vessel Identification Number."; vid
INPUT "Enter the Test Identification Number."; tid
INPUT "Enter the Trigger Level for The Oscilloscope."; triglev
INPUT "Enter the Range for Channel 1 of the Oscilloscope."; rngch1
INPUT "Enter the X coordinate for the Recording Sensor."; sens1x
INPUT "Enter the Y coordinate for the Recording Sensor."; sens1y
INPUT "Enter the X coordinate for the Trigger Sensor."; sens2x
INPUT "Enter the Y coordinate for the Trigger Sensor."; sens2y
```

```
*****
'Configure Personnal488 card
```

```
OPEN "\DEV\IEEEOUT" FOR OUTPUT AS #1
IOCTL #1, "BREAK"           'reset gpib card
PRINT #1, "RESET"
OPEN "\DEV\IEEEIN" FOR INPUT AS #2
PRINT #1, "FILL ERROR"
ON ERROR GOTO ieeer
PRINT #1, "ERROR OFF"
```

```
*****
'Configure Keithley 197 Digital Multi Meter (Address 20)
'sets default configuration function, range front panel
'relative off, db off trigger continuous on talk data format
'with prefix EOI enabled, srq terminator carriage return
'data logger disabled
```

```
PRINT #1, "OUTPUT 20; CLEAR"
PRINT #1, "REMOTE 20"
PRINT #1, "OUTPUT 20; T1X"
```

```

*****
'Configure HP 54601A Oscilloscope (Address 07)
'Reset scope to default, see page 7-14 of HP manual for
'details on default values.
'
  PRINT #1, "OUTPUT 07; *RST"
  PRINT #1, "OUTPUT 07; :TIM:RANG .2 MS;REF LEFT"
  PRINT #1, "OUTPUT 07; :TRIG:MODE SINGLE;SOUR CHAN2;LEV 8.75 mV"
  PRINT #1, "OUTPUT 07; :CHAN1:COUP AC;RANG .16 V"
  PRINT #1, "OUTPUT 07; :CHAN2:COUP AC;RANG .16 V"
  PRINT #1, "OUTPUT 07; :ACQ:TYPE NORMAL;COMPLETE 80"
  PRINT #1, "OUTPUT 07; :DITHER OFF"
cycle = 0
nw = 0
*****
'The RUN statement configures the scope to wait for a trigger level
'exceedance so that it can store the signal in case it occurs
'The loop keeps checking if the scope has triggered while it also
'checks the voltmeter reading. Once trigger occurs, the waveform
'is stored by (waveget:). If the scope is not triggered before the
'voltage drops below 90%, the scope is stopped and the program is
'returned to dmm:
'
trigger:
  PRINT #1, "OUTPUT 07;;run"
  WHILE vtlvl >= 0
    IF vtlvl < 1 THEN flag = 0
    PRINT #1, "OUTPUT 07;*CLS"
    PRINT #1, "OUTPUT 07;*ESE 2"           'enables trigger register'
    PRINT #1, "OUTPUT 07;:TER?"         'queries trigger event'
    PRINT #1, "ENTER 07"
    vtwave = 0
    WHILE IOCTL$(2) = "1"
      vttrg = VAL(INPUT$(1, 2))
      IF vttrg = 1 THEN vtwave = 1
    WEND
    IF vtwave = 1 THEN GOTO waveget
  WEND

  PRINT #1, "ENTER 20"           'read voltage from dmm
  INPUT #2, v$
  vtlvl = VAL(MID$(v$, 5, LEN(v$)))
  IF vtlvl > 1 THEN GOSUB count:
  WEND
'
*****

```

'These commands digitize and store the waveform in channel 1 on
'the virtual disk D:

waveget:

```

nw = nw + 1
tload = (vtlvl * 332) - 302
vread = vtlvl
OPEN "A", 3, "D:\CNT" + LTRIM$(STR$(vid)) + LTRIM$(STR$(tid)) + ".DAT"
PRINT #3, "wave"; nw; " at cycle"; cycle; " load="; tload; " psi"
CLOSE #3
file$ = "D:\\" + LTRIM$(STR$(vid)) + LTRIM$(STR$(tid)) + "w" +
LTRIM$(STR$(nw)) + ".dat"
OPEN "O", 4, file$
PRINT #4, TIME$ + " " + DATE$
PRINT #4, nw
PRINT #4, tload
PRINT #4, vid
PRINT #4, tid
PRINT #4, samplerate
PRINT #4, lengthfile
PRINT #4, triglevel
PRINT #4, sens1x
PRINT #4, sens1y
PRINT #4, sens2x
PRINT #4, sens2y
PRINT #4, 8
PRINT #4, 128
PRINT #4, rngchl
PRINT #4, "WDI-21"
PRINT #4, "sens2id"
PRINT #4, 0
PRINT #4, 0
PRINT #4, 0
iw = 0
PRINT #1, "OUTPUT 07; :WAV:POIN 2000;FORM BYTE;SOUR CHAN1"
PRINT #1, "OUTPUT 07; :WAV:DATA?"
PRINT #1, "ENTER 07"
WHILE IOCTL$(2) = "1"
  iw = iw + 1
  wave$(iw) = INPUT$(1, 2)
  PRINT #4, wave$(iw);
WEND
CLOSE #4
PRINT "wave"; nw; " at cycle"; cycle; " load = "; tload; " psi"
IF nw > 500 THEN BEEP

```



```
IF nw = 520 THEN STOP
GOTO trigger:
ieeer:
  IOCTL #1, "BREAK"
  PRINT #1, "STATUS"
  INPUT #2, ST$
  PRINT CHR$(7); "Error #"; MID$(ST$, 15, 2); ": "; MID$(ST$, 27)
  STOP'RESUME NEXT
  END
count:
  IF flag = 0 THEN cycle = cycle + 1
  flag = 1
  RETURN
```

APPENDIX B
NOISE.BAS, BASIC COMPUTER PROGRAM

```

CLS
DIM BUMB!(2000)
INPUT "ENTER THE VESSEL ID NUMBER.", VID%
INPUT "ENTER THE TEST ID NUMBER", TID%
INPUT "ENTER THE STARTING WAVE NUMBER.", STWV%
INPUT "ENTER THE FINAL WAVE NUMBER.", FINAVW%
INPUT "ENTER THE STARTING WAVE NUMBER FOR THE OUTPUT", LK%
FOR I% = STWV% TO FINAVW%
  FILE$ = "C:\TESTMAT\11N" + LTRIM$(STR$(I%)) + ".DAT"
  OPEN FILE$ FOR INPUT AS #1
  FOR J% = 1 TO 1999
    INPUT #1, BUMB!(J%)
    IF BUMB!(J%) >= .016 THEN
      MIND% = 1
    END IF
    IF BUMB!(J%) <= 0! THEN
      LOWIN% = 1
    END IF
    IF J% >= 1750 THEN
      IF BUMB!(J%) = BUMB!(1) THEN
        K% = J%
        KONE% = 1
      END IF
    END IF
    IF MIND% = 1 AND LOWIN% = 1 THEN
      IF KONE% = 1 THEN J% = 1999
      LONE% = 1
    END IF
    IF EOF(1) THEN J% = 1999
  10 NEXT J%
  IF LONE% = 1 THEN
    FILE1$ = "C:\TESTFAT\" + LTRIM$(STR$(VID%)) + LTRIM$(STR$(TID%)) + "F"
    + LTRIM$(STR$(LK%)) + ".DAT"
    OPEN FILE1$ FOR OUTPUT AS #2
    FOR L% = 1 TO K%
      WRITE #2, BUMB!(L%)
    NEXT L%
    CLOSE #2
    FIL2$ = "C:\TESTFAT\V" + LTRIM$(STR$(VID%)) + "T" +
    LTRIM$(STR$(TID%)) + ".COR"
  
```

```
OPEN FIL2$ FOR APPEND AS #3
FIL3$ = "C:\TESTMAT\" + LTRIM$(STR$(VID%)) + LTRIM$(STR$(TID%)) +
"W" + LTRIM$(STR$(I%)) + ".DAT"
PRINT #3, "ORIGINAL FILE NAME "; FILE$
PRINT #3, "NEW FILE NAME "; FILE1$
PRINT #3, " "
CLOSE #3
LK% = LK% + 1
END IF
CLOSE #1
LOWIN% = 0
K% = 0
LONE% = 0
MIND% = 0
KONE% = 0
NEXT I%
PRINT "THE NUMBER OF WAVES SAVED IS ", LK%
END
```